ACS APPLIED BIO MATERIALS

www.acsabm.org

Review

Recent Advances in Self-Assembled DNA Nanostructures for Bioimaging

Qi Yang, Xu Chang, Jung Yeon Lee, Tiffany Olivera, Minu Saji, Henry Wisniewski, Suchan Kim, and Fei Zhang*

Cite This: https://doi.org/10.1021/acsabm.2c00128

Read Online

ACCESS | Metrics & More | Article Recommendations

ABSTRACT: DNA nanotechnology has proven to be a powerful platform to assist the development of imaging probes for biomedical research. The attractive features of DNA nanostructures, such as nanometer precision, controllable size, programmable functions, and biocompatibility, have enabled researchers to design and customize DNA nanoprobes for bioimaging applications. However, DNA probes with low molecular weights (e.g., 10−100 nt) generally suffer from low stability in physiological buffer environments. To improve the stability of DNA nanoprobes in such environments, the DNA nanostructures can be designed with relatively larger sizes and defined shapes. In addition, the established modification methods for DNA nanostructures are also essential in enhancing their properties and performances in a physiological environment. In this review, we begin with a brief recap of the development of DNA nanostructures including DNA tiles, DNA origami, and multifunctional DNA nanostructures with modifications. Then we highlight the recent advances of DNA nanostructures for bioimaging, emphasizing the latest developments in probe modifications and DNA-PAINT imaging. Multiple imaging modules for intracellular biomolecular imaging and cell membrane biomarkers recognition are also summarized. In the end, we discuss the advantages and challenges of applying DNA nanostructures in bioimaging research and speculate on its future developments.

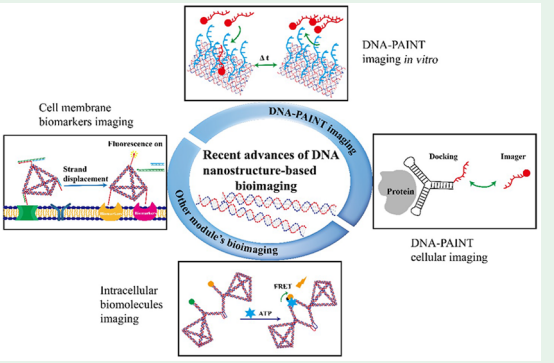

KEYWORDS: *DNA nanotechnology, DNA-PAINT imaging, bioimaging modules, biomolecules, cellular imaging, in vitro*

1. INTRODUCTION

Bioimaging is an essential technique to provide intuitive and multidimensional information for disease diagnosis, cancer treatments, and basic pathological studies. A good number of imaging techniques are used for clinical trials including magnetic resonance imaging (MRI), fluorescence imaging (FLI), positron emission tomography (PET), computed tomography (CT), single-photon emission computed tomography (SPECT), and optical super-resolution imaging. Although imaging methods vary, the requirements for ideal imaging probes, such as low toxicity and cost, high signal-to-noise ratio, and biocompatibility, remain consistent. However, it is still challenging to fabricate an imaging probe with ideal size, shape, stability, and compatibility.[1]

DNA has been exploited as a building material to construct nanoscale architectures based on Watson−Crick base pairing. The control over its shape, size, and dimension can be achieved by sequence design and oligonucleotides arrangement, allowing the creation of almost any arbitrary architecture from one-dimensional (1D), two-dimensional (2D) arrays, and even three-dimensional (3D) crystals with atomic precision.[2] DNA nanostructure materials provide unique templates for the precise arrangement of guest molecules and functional materials with defined numbers and addresses.[3] For example, small molecules such as dyes, drugs, peptides, and proteins have been integrated with DNA nanostructures with accurate amounts and locations as diagnostic imaging or therapeutic DNA nanodevices. Furthermore, reconfigurable DNA nanostructures perform dynamic switching in response to specific stimuli, showing their usage in biomolecular sensing and imaging. Here, we first list a general timeline of structural DNA nanotechnology (Figure 1) and discuss the recent strategies for constructing DNA nanostructure-based probes and labels for bioimaging applications. In particular, we will focus on the current developments of DNA-based point accumulation for imaging in nanoscale topography (DNA-PAINT) imaging *in*

Special Issue: Self-Assembling Biomaterials from Proteins, Peptides, and DNA

Received: February 13, 2022
Accepted: April 28, 2022

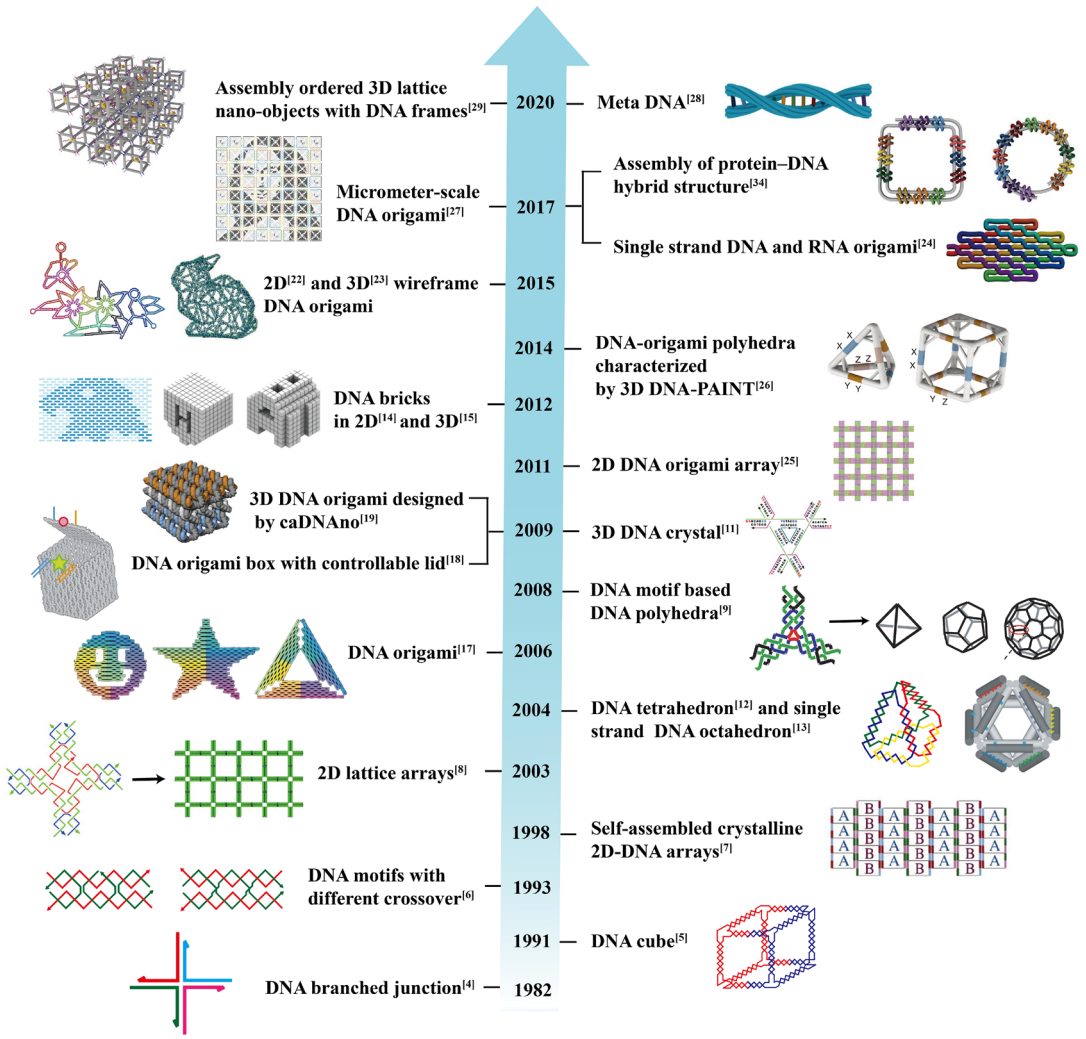

Figure 1. Brief timeline of the development of structural DNA nanostructures. DNA branched junction.[4] DNA cube.[5] DNA motifs with different crossover.[6] Self-assembled crystalline 2D-DNA arrays. Reproduced with permission from ref 7. Copyright Springer Nature 1998. 2D lattice arrays. Reproduced with permission from ref 8. Copyright Association for the Advancement of Science (AAAS) 2003. DNA tetrahedron.[12] Single-stranded DNA octahedron. Reproduced with permission from ref 13. Copyright Springer Nature 2004. DNA origami. Reproduced with permission from ref 17. Copyright Springer Nature 2006. DNA motif-based DNA polyhedral. Reproduced with permission from ref 9. Copyright Springer Nature 2008. 3D DNA crystal. Reproduced with permission from ref 11. Copyright Springer Nature 2009. DNA origami box with controllable lid. Reproduced with permission from ref 18. Copyright Springer Nature 2009. 3D DNA origami designed by caDNAno. Reproduced with permission from ref 19. Copyright Springer Nature 2009. 2D DNA origami array. Reproduced with permission from ref 25. Copyright Wiley-VCH 2011. DNA bricks in 2D. Reproduced with permission from ref 14. Copyright Springer Nature 2012. DNA bricks in 3D. Reproduced with permission from ref 15. Copyright AAAS 2012. DNA-origami polyhedral characterized by 3D DNA-PAINT. Reproduced with permission from ref 26. Copyright AAAS 2014. 2D wireframe DNA origami. Reproduced with permission from ref 22., Copyright Springer Nature 2015. 3D wireframe DNA origami. Reproduced with permission from ref 23. Copyright Springer Nature 2015. Single strand DNA and RNA origami. Reproduced with permission from ref 24. Copyright AAAS 2017. Assembly of protein−DNA hybrid structure. Reproduced with permission from ref 34. Copyright AAAS 2019. Micrometre-scale DNA origami. Reproduced with permission from ref 27. Copyright Springer Nature 2017. Meta DNA. Reproduced with permission from ref 28. Copyright Springer Nature 2020. Assembly ordered 3D lattice nano-objects with DNA frames. Reproduced with permission from ref 29. Copyright Springer Nature 2020.

vitro and the recent studies of modified DNA nanostructures for cellular and *in vivo* imaging.

2. SELF-ASSEMBLED DNA NANOSTRUCTURES

2.1. DNA Tiles. The concept of DNA nanotechnology was first proposed by Ned Seeman in 1982.[4] He proposed the use of several short single-stranded DNA oligos to self-assemble into an immobile Holliday Junction (HJ) tile through hybridization. By employing sticky-end interactions between tiles, HJ DNA tiles can be linked with each other through complementary sequences to form 2D arrays. In 1991, Seeman and co-workers demonstrated a self-assembled DNA cube.[5] To increase the rigidity of the DNA tile, Seeman et al. designed the DNA double-crossover molecule (DX) by introducing two crossovers between two DNA double helices.[6] Later on, Erik and co-workers successfully self-assembled DNA 2D arrays based on DX tiles using programmable sticky-ends.[7] In 2003, Yan et al. extended the DX tiles to a more rigid DNA 4 × 4 tile with four arms pointing to different directions.[8] They used a long central strand to tighten the four arms together into one tile, and the monomer tiles could be assembled into nanoribbons and 2D grid-like lattices. After this, small

https://doi.org/10.1021/acsabm.2c00128
ACS Appl. Bio Mater. XXXX, XXX, XXX−XXX

repeating DNA motifs that were assembled into 2D and 3D lattices have been reported. For example, He et al. presented the polyhedral nanostructures assembled from fixed numbers of DNA three-arm junction motifs.[9] These three-arm junction tiles were programmable and easily modified. They could serve as a novel platform to carry biological and inorganic nanocomponents to form 2D or 3D arrays with precise control in nanoscale. Carter et al. reported that peptides could recognize and bind with gold nanoparticles and generate a self-assembled superstructure of DNA peptides and gold nanoparticles by integrating peptide-coupled DNA with the 4 × 4 cross-tile system.[10] Furthermore, Zheng et al. proposed the self-assembled 3D crystal with 4 Å resolution based on the DNA tensegrity triangle tiles.[11]

More recently, Goodman et al. presented a DNA tetrahedral nanostructure by annealing four properly designed single strands together.[12] This nanostructure had excellent rigidity and adaptability, showing great potential to cage other molecules. Around the same time, Shih et al. reported an octahedron-shaped DNA nanostructure constructed mainly by a 1.7-kilobase single-stranded DNA scaffold.[13] The scaffold is bound with five 40-nucleotide staples to form a branched arm structure, connected by paranemic-cohesions at the end of each arm. Later, to assemble finite and more complex 2D and 3D structures, the Yin group first proposed the "DNA bricks" concept.[14] The DNA bricks are single-stranded tiles (SST), consisting of defined lengths of single DNA strands with different sequences composed entirely of concatenated sticky ends. Each strand would bind to four local neighbors during annealing and finally grow into complex 2D and 3D shapes.[14,15] Notably, with the precise design of sequence and connection, 3D nanostructures such as a teddy bear, a bunny, and a helicoid were achieved as well.[16]

2.2. DNA Origami. In 2006, Paul Rothemund reported a novel DNA origami method for DNA self-assembly.[17] He used a long single-stranded DNA as a scaffold and mixed it with hundreds of short DNA oligos as staples to self-assemble into a defined shape. The intrinsic composition of DNA origami allowed the design of different structures with molecular precision by manipulating the sequence. On this basis, a variety of prescribed 2D shapes with different sizes have been constructed including a triangle, a rectangle, a smiley face, and a star. Following this, Andersen et al. extended the 2D DNA origami method into 3D structures designing by creating a box-shaped DNA origami structure with a controllable lid in 2009.[18] This DNA box had a large cavity that could be filled with a ribosome or a poliovirus. This device had the potential to sense or deliver biomolecular targets for *in vivo* therapeutic applications. In the meantime, Douglas et al. developed a software, caDNAno.[19] With the help of caDNAno, they designed many 3D DNA origami shapes with precisely controlled dimensions ranging from 10 to 100 nm including a monolith, a square nut, a railed bridge, a genie bottle, a stacked cross, and a slotted cross.[20] Moreover, they successfully fabricated twisted or curved DNA bundles with quantitatively controlled angles by manipulating the insertions and deletions of base pairs.[21] After that, the development of wireframe structures made the origami family more extensive. For example, the 2D wireframe patterns including a star, a Penrose tiling, a wavy grid, a fishnet, and a flower-and-bird pattern were reported by Zhang et al.,[22] and the 3D wireframe structures, such as icosahedron, a rod, a waving stickman, a bottle, and a bunny, were presented by Benson et al.[23] Compared with traditional tightly packed DNA origami structures, the wireframe structures would be easily incorporated with mechanical springs or tensegrity properties into the addressable edges to construct responsive nanodevices. Furthermore, Han et al. designed and synthesized an unknotted compact origami structure with a long single DNA or RNA strand, demonstrating facile replication of the strand *in vitro* and in living cells.[24]

All the origami units discussed above have defined size and good monodispersibility. However, the scale of DNA origami is limited by the length of the scaffold. To assemble larger DNA structures, the primary method is connecting the monodispersed origami units into large periodic lattices. There are two types of general methods of gluing origami units together. One method is using sticky-end connections based on sequence-specific base pairings between origami monomers. The connection between DNA origami monomers is precisely designed with unique interactions. For instance, Liu et al. constructed a cross-shaped origami tile and assembled large 2D lattices through sticky end binding.[25] Yin's group reported a stiff DNA origami "tripod" monomer with precisely controlled arm lengths and interarm angles for the hierarchical self-assembly of polyhedrons.[26] The tripod monomers were bound through sticky ends and were precisely assembled into the target tetrahedron and hexagonal structure. Later, Tikhomirov et al. produced the DNA origami arrays with sizes up to 0.5 square micrometer by tuning the number of weak sticky end interactions on each edge, allowing the rendering of images such as the Mona Lisa and a rooster.[27] More recently, Yao et al. proposed the "Meta DNA" concept to assemble diverse and complex structures on the micrometer scale based on the specific base pairing between different DNA six-helix bundles.[28] Meanwhile, Tian et al. assembled polyhedral origami structures into multiple superlattice frameworks by introducing several single linker strands with sticky ends to the vertex of the DNA origami structures and cocrystallized them with nanoparticles of different compositions.[29] Additionally, assigning protruding strands to predefined positions enabled the polyhedral origami structures to be filled with gold nanoparticles with high efficiency and addressability, which is meaningful for the orderly arrangement of inorganic nanoparticles.

The second strategy to connect DNA origami monomers is using base-stacking interactions of blunt ends from parallel DNA helices. In 2011, Rothemund et al. proposed that the geometric arrangement of blunt-end stacking interactions could help create varied bonds.[30] They programmed the blunt end stacking interactions into binary, or shape codes, to achieve specific hybridization. More recently, Gerling et al. discussed the rules of shape complementarity to specifically self-assemble discrete 3D DNA components.[31] They found that the base stacking interactions could stabilize the origami units' assembly by counteracting electrostatic repulsion between component interfaces. Furthermore, the balance between stacking force and electrostatic repulsion of DNA was susceptible to changes in ion concentration and temperature. By adjusting the Mg^{2+} concentration and temperature, they controlled the interaction between the origami units switching between "on" and "off" states.

2.3. Modifications of DNA Nanostructures. DNA nanostructures made of pure DNA strands generally have limited applications due to the inherent properties of the DNA material. To increase the diversity of functional DNA

https://doi.org/10.1021/acsabm.2c00128
ACS Appl. Bio Mater. XXXX, XXX, XXX−XXX

nanostructures, a wide variety of materials have been introduced and modified on DNA including small organic molecules (dyes), proteins, and inorganic nanoparticles. The key to modifying DNA with other materials lies in creating connections between DNA and the guest materials. These connections can be covalent, noncovalent, or electrostatic binding. As we know, nucleotides are the basic building blocks to create a DNA strand, and each of them consists of three subunits: a nitrogenous base, a five-carbon sugar moiety, and a phosphate backbone. The functional groups on these subunits provide a lot of reaction possibilities for chemical modifications of DNA nanostructures. DNA strands as anionic polymers can also electrostatically bind with ionic polymers or particles that tremendously broaden the diversity of guest materials.

Small molecules can directly react with a nucleotide and generate covalent connection. For example, generating covalent bonds between DNA and dyes is an efficient and reliable method.[32] DNA can be tracked and visualized after their modification with dye molecules, allowing the sensing and imaging of specific targets based on DNA recognition. Moreover, DNA origami structures are known to have high addressability. Researchers can randomly select specific locations and seed the dye molecules on them. By doing so, only a small amount of the dye molecules needs to be loaded, and fluorescent quenching induced by dye aggregation can be avoided.[33]

DNA−protein conjugates can be formed by a covalent connection between DNA and protein. For example, Biotinylated oligonucleotide is a typical conjugate with a covalent bond, which has high production yield and becomes a commercial DNA−protein conjugated product. An early example of DNA tiles consisting of biotinylated oligonucleotides was reported in 2003 by Yan et al.[8] The biotinylated oligonucleotides were preassembled into 4 × 4 DNA tiles and then into a 2D lattice by base pairing. By exploiting biotin−streptavidin specific interactions and the DNA 2D lattice template, they could assemble a periodic protein array. Some proteins can specifically bind with unique DNA sequences, bringing new insight into DNA−protein conjugates production and bioimaging application. Praetorius et al. proposed a new approach to combining the DNA strands with proteins by specific sequence binding.[34] They customized a set of staple proteins to recognize and link two distinct double-helical DNA sequences at different positions on a DNA template, thus folding a double stranded DNA template into a user-defined shape. More recently, researchers found that small structures like aptamers, peptides, and enzymes can selectively capture the target proteins with high affinity. This selective binding with target proteins opened a new way for recruiting multiple proteins onto DNA nanostructures. For example, Li et al. constructed a thrombin-loaded origami structure with its edges locked by AS1411 DNA aptamer.[35] Overexpressed nucleolin binding could open the AS1411 aptamer 'lock' when the locked-state origami structure approached the target tumor site *in vivo*. Then the loaded thrombin molecules were exposed, which induced coagulation inside of blood vessels, thus forming intravascular thrombosis and inhibiting tumor growth.

Various inorganic nanoparticles such as silver nanoparticles, gold nanoparticles, lanthanide-doped upconversion nanoparticles (UCNPs), and iron oxide nanoparticles have been modified onto DNA nanostructures by electrostatic binding. With the help of the magnetic or optical features of these nanoparticles, DNA nanostructures can be adapted to different imaging modules. The connection between DNA and nanoparticles is mainly based on chemical bonds or electrostatic attraction. For example, Ge et al. reported the method of creating DNA-modified UCNPs.[36] These conjugate nanoparticles had a luminescent UCNP core, which exhibited great potential as multifunctional imaging agents or therapeutic candidates for biomedical applications.

3. DNA-PAINT TECHNIQUE AND ITS RECENT ADVANCES

Over the past decade, developments in fluorescence super-resolution microscopy have enabled the visualization of biological systems at the molecular scale with unprecedented high resolutions. DNA-PAINT can achieve super-resolution imaging by using the stochastic and transient binding of fluorescently labeled DNA probes. DNA-PAINT also can be easily implemented on any sensitive wide-field fluorescence microscope without further modification.[37] However, current DNA-PAINT strategies have some limitations such as low throughput and excessive acquisition time. In this section, we will briefly review the DNA-PAINT technique and discuss the recent progressions and applications of this technique for *in vitro* and cellular imaging.

3.1. Brief Introduction of DNA-PAINT Imaging. DNA-PAINT imaging is a super-resolution imaging method based on capturing blinking signals generated by transient binding and unbinding between short dye-labeled DNA oligonucleotides. During imaging, the targets are labeled with a short DNA strand acting as immobilized "docking sites", while a complementary DNA strand is labeled with a dye molecule as a free "imager" in solution. When the imager strand is hybridized with the docking sites, an increased fluorescence signal, an "on" state, was observed. In contrast, a decreased fluorescence signal, an "off" state, would be found after the imager strand left the "docking sites". The fluorescence signals of the nanoscale targets were visualized in real-time with the acquired data being readily analyzed.

With the development of DNA nanotechnology, a DNA origami structure can serve as a substrate with suitable docking sites for DNA-PAINT *in vitro* imaging, owing to its programmability and spatial addressability. In 2010, Jungmann et al. first demonstrated a DNA-PAINT technique with DNA origami substrates as docking sites.[37] They constructed a 2D long rectangular origami structure with three, spaced apart, docking strand sites (∼130 nm). Small dye-labeled DNA imager strands are reversibly and specifically hybridized with the docking strands on the surface of DNA origami structures. The precise and transient interactions between the docking strands and the imager strands enabled the locating of the docking sites on the origami surface. Furthermore, DNA-PAINT imaging has also been used for the visualization of 3D origami structures in solution. For example, Iinuma et al. designed a stiff three-arm-junction DNA origami tile motif with precisely controlled arm lengths and angles for the hierarchical assembly of polyhedral 3D structures including tetrahedrons, triangular prisms, cubes, pentagonal prisms, and hexagonal prisms.[26] They successfully characterized these near-solution shaped 3D origami structures with DNA-PAINT imaging. Unlike the Cryo-EM, which relies on a class of images averaging, DNA-PAINT is a relatively straightforward and fast technique to obtain real-time images of individual 3D structures.

https://doi.org/10.1021/acsabm.2c00128
ACS Appl. Bio Mater. XXXX, XXX, XXX−XXX

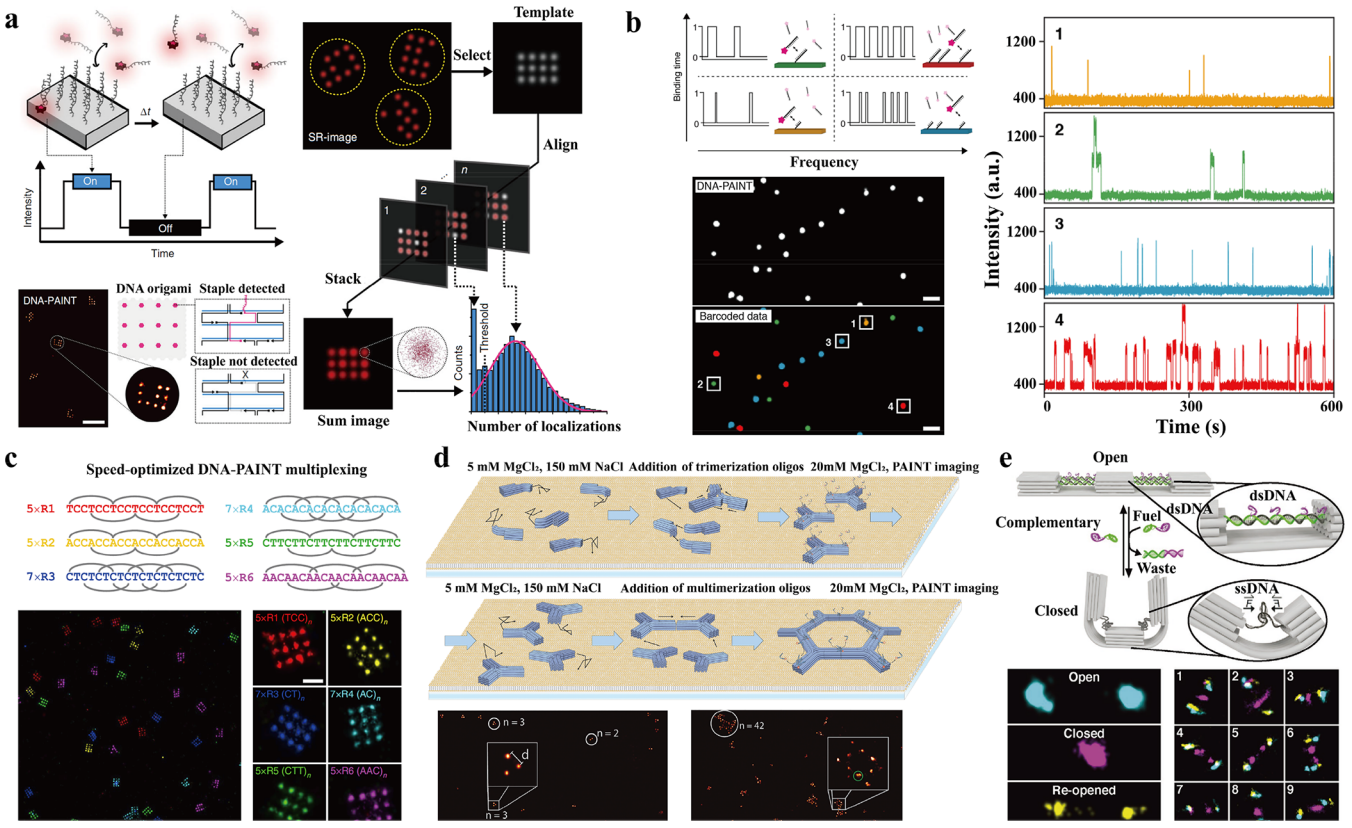

Figure 2. Recent technique developments of DNA-PAINT imaging *in vitro*. (a) Quantitative analysis of staples in origami via DNA-PAINT imaging including the concept of DNA-PAINT and the general workflow for assessing the abundance of docking sites. Reproduced with permission from ref 40. Copyright Springer Nature 2018. (b) Multiplexed DNA-PAINT imaging by engineering blinking kinetics allows the creation of "barcodes" for simultaneous multiplexing and only using a single imager strand species. Reproduced with permission from ref 42. Copyright American Chemical Society 2019. (c) Design and proof-of-concept experiments of concatenated speed-optimized motifs (the six orthogonal binding motifs) for multiplexing in Exchange-PAINT experiments. Reproduced with permission from ref 44. Copyright Springer Nature 2020. (d) Process of stop-and-go assembly of triskelion structures and hexagonal lattices and the corresponding DNA-PAINT images. Reproduced with permission from ref 45. Copyright American Chemical Society 2019. (e) Overview of the DNA origami switch design and visualization of the different states of individual switches by DNA-PAINT imaging. Reproduced with permission from ref 46. Copyright Wiley-VCH 2021.

Visualizing several distinct cellular species is difficult to implement with the traditional DNA-PAINT technique. Jungmann et al. proposed the idea of Exchange-PAINT imaging for cellular structure detection.[38] On the basis of multiplexed-PAINT, orthogonal sequences were employed to label distinct docking sites to achieve imaging specificity. The multiplexing approach could be adjusted by tuning the binding strength and concentration of the imager strands, allowing the sequential imaging of multiple targets with only a single dye molecule and a single laser source. Exchange-PAINT is a new multiplexing approach in which the imager strands are sequentially applied to recognize the different targets on the same sample. In each round of imaging, only one imager strand was introduced to capture the specific target docking sites, followed by a washing step to remove the imager strand. The imaging and washing steps were repeated until all desired targets were imaged, and the multicolor image of the target sample was produced after aligning and combining the collected images. In the end, they achieved the multiplexed 2D and 3D DNA-PAINT imaging of different protein components in fixed cells by linking DNA-PAINT docking strands to antibodies.

One of the problems in obtaining the super-resolution images of thick biological samples is the requirement of increasingly complex hardware. Schueder et al. combined the 3D DNA-PAINT with a spinning disk confocal (SDC) hardware to overcome the sample thickness limitation for imaging.[39] They demonstrated that this method could be applied to imaging the interior of cells for various cellular targets including DNA, RNA, and proteins. The multiplexed 3D super-resolution imaging at sample depths of up to ~10 μm could achieve resolution as much as 20 nm planar and 80 nm axial, leading to the high-resolution DNA-PAINT technique for whole cell imaging.

3.2. Applications of DNA-PAINT Imaging *In Vitro*.

A DNA origami structure with great programmability and addressability can serve as a suitable docking site for DNA-PAINT imaging. Using DNA nanostructures as docking sites are classified as DNA-PAINT imaging *in vitro*. The latest progress of *in vitro* DNA-PAINT imaging will be discussed with emphasis on the quantitative analysis of docking sites' binding rates, multiplexing imaging, acquisition efficiency improvement, and dynamic motion observation.

DNA strands can be modified with functional entities and assembled into functionalized DNA nanostructures. However, the quantification and efficiency of functional entity attachments are less studied. As shown in Figure 2a, Strauss et al. used DNA-PAINT to quantify both the incorporation and accessibility of all individual strands in a DNA origami structure with molecular resolution in 2018.[40] They found

https://doi.org/10.1021/acsabm.2c00128
ACS Appl. Bio Mater. XXXX, XXX, XXX−XXX

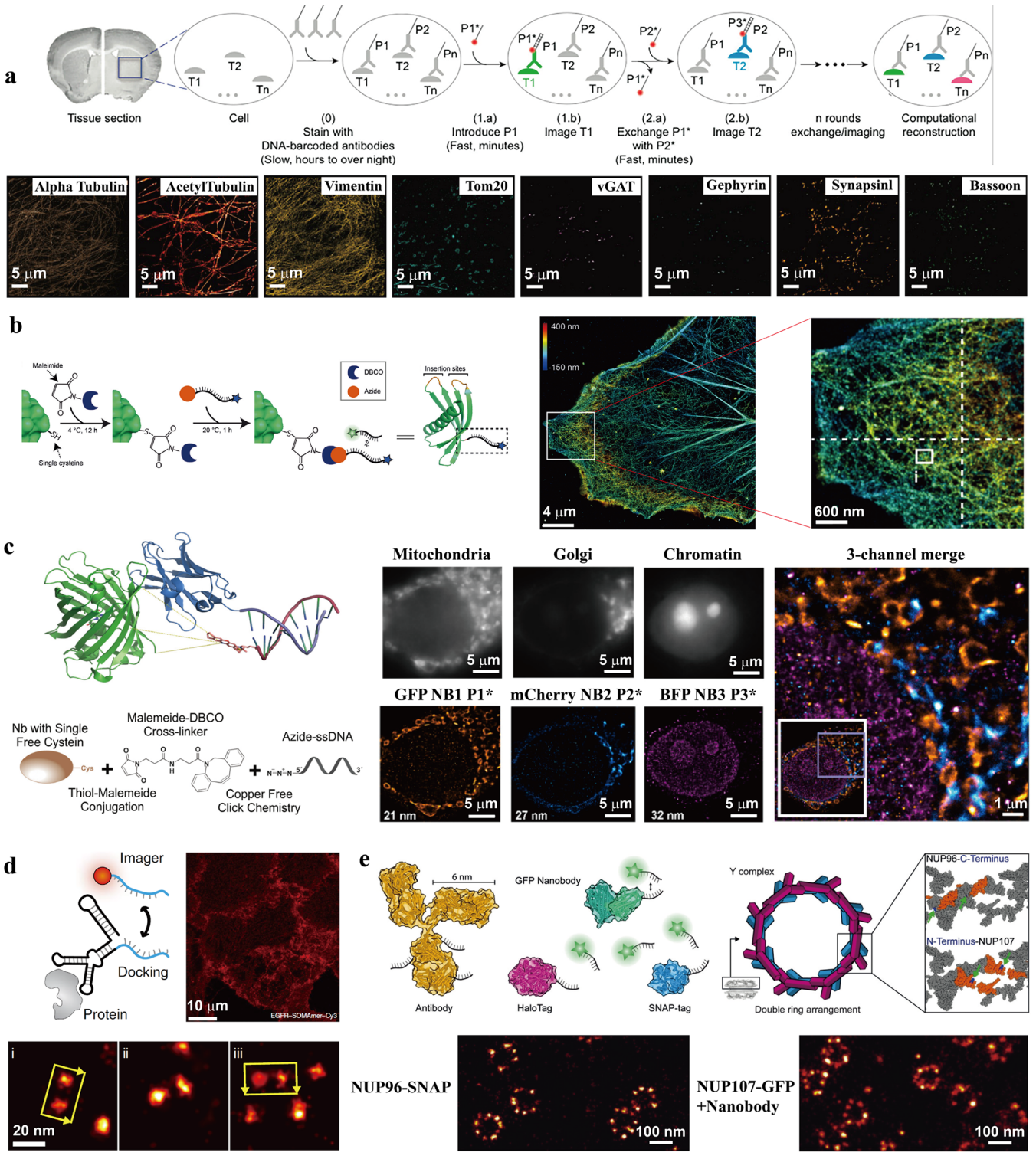

Figure 3. Recent advances of DNA-PAINT technique in cellular imaging. (a) Schematic of DNA exchange imaging and its application for the imaging of eight-target proteins in primary neurons. Reproduced with permission from ref 48. Copyright American Chemical Society 2017. (b) Site-specific DNA labeling of Affimer reagents and DNA-PAINT images of actin filaments in a Cos7 cell. Reproduced with permission from ref 49. Copyright Wiley-VCH 2018. (c) Click- and thiol-based strategy to conjugate nanobodies to a docking DNA strand and exchange PAINT imaging of individual target fluorophores. Reproduced with permission from ref 50. Copyright Wiley-VCH 2021. (d) Quantitative, high-resolution DNA-PAINT imaging of SOMAmer labeling probes for EGFR targeting. Reproduced from with permission from ref 52. Copyright Springer Nature 2018. (e) Genetically encoded self-labeling enzymes modified DNA strands for DNA-PAINT imaging of NUP96 proteins. Reproduced with permission from ref 53. Copyright Elsevier 2019.

that the strand incorporation rates were strongly correlated with the position of docking sites inside of the DNA origami structure, ranging from a minimum of 48% on the edges to a maximum of 95% in the center. This work provided a good example for quantitative analysis of the docking sites' binding rates, which may also apply to the characterization of the

https://doi.org/10.1021/acsabm.2c00128
ACS Appl. Bio Mater. XXXX, XXX, XXX−XXX

labeling efficiency of antibodies, nucleic acids, and other cellular components. Then Hahn et al. applied DNA-PAINT to visualize the availability of handle sites and leash sites on a catenane DNA template.[41] This revealed that the availability of programmed handles was measured to be 93%, which was consistent with previously reported yields,[40] indicating DNA-PAINT as a reliable, quantitative analysis method.

A high acquisition efficiency is necessary for exploring the detailed molecular workings of complex cellular machinery. However, the early staged multiplexed DNA imaging required a very long acquisition time due to the single type of fluorophore and sequential imaging processing cycles.[38] To improve the acquisition speed, Wade et al. introduced a new barcoding approach for multiplexed DNA-PAINT imaging by modulating the binding kinetics of transient hybridization.[42] As shown in Figure 2b, they designed DNA origami structures as docking sites and assigned multiple binding sites to single origami surfaces for analyzing the kinetic barcoding approach *in vitro*. The binding kinetics of programmable DNA probes, such as blinking frequency and duration, were tuned precisely and used downstream as barcodes for multiplexed detection enabling hundreds or more targets to be imaged simultaneously. As a result, DNA-PAINT was able to reach 124-plex within minutes *in vitro* and *in situ*. Besides, Schueder et al. demonstrated that one can design and optimize DNA sequences and buffer conditions to improve the acquisition speed. In this way, DNA-PAINT could achieve an order of magnitude faster imaging speed without compromising image quality or spatial resolution either *in vitro* with DNA origami or *in situ* using cell samples.[43] However, this improvement did not reach the ultimate speed limit and was only applicable for single target imaging. Therefore, Strauss et al. recently introduced concatenated periodic DNA sequence motifs to further improve the acquisition speed, leading up to a 100-fold imaging speed amplification compared to the traditional DNA-PAINT.[44] As shown in Figure 2c, they applied this method in six orthogonal sequence models. Each of the sequences contained five or seven pieces of overlapping motifs, which were complementary with corresponding imager strands. This method achieved speed-optimized multiplex imaging with lower imager concentrations and improved the signal-to-noise ratio.

DNA-PAINT imaging as a solution-based super-resolution imaging technique provides a valuable tool for observing the dynamic process of binding and unbinding between docking sites and imager strands. Recently, DNA nanostructure-based dynamic devices have been studied as convenient models to explore nanoscale dynamic assembly progress. For example, Kempter et al. found that the behavior of DNA nanostructures and their assembly into higher-order membrane-bound lattices can be controlled in a stop-and-go manner. DNA-PAINT imaging was used to monitor the dynamic process of the DNA nanostructure assembly into lattices.[45] As shown in Figure 2d, they designed DNA triskelions and transiently immobilized them on glass-supported lipid bilayers by changing the mono- and divalent cation concentrations inside the surrounding buffer. Then they exchanged the buffer and added another set of oligonucleotides, which triggered the triskelions to diffuse and assemble into hexagonal 2D lattices. This work provided an excellent example in the controlling and observation of the diffusion behavior of DNA nanostructures on lipid membranes. Recently, Gür et al. fabricated a self-assembled DNA origami switch that utilized a strand displacement reaction to achieve an internally reversible conformational change.[46] In Figure 2e, the open and closed states of a DNA origami structure were clearly observed by DNA-PAINT imaging based on the transition between double-stranded and single-stranded DNA. The nine different overlay images of the three imaging rounds indicated good repeatability in the switching of the origami structure between the two states. The dynamic states of DNA origami structures also demonstrated their continuous configuration variability in solution. In addition, Scheckenbach et al. applied the DNA-PAINT technique to monitor the self-regeneration and self-healing of DNA origami nanostructures.[47] The reconfiguration of DNA origami nanostructures induced by the self-repair of enzymatic damage and photo-induced defects could be intuitively visualized by DNA-PAINT imaging.

3.3. Applications of DNA-PAINT Technique for Cellular Imaging. Imagers and DNA docking sites are required to be labeled with small and efficient labeling molecules for high spatial resolution observation of cellular targets. Multifunctional DNA nanostructures provide more options for the designing of imagers and docking sites. Generally, dyes, antibodies, genetically encoded self-labeling enzymes, and DNA aptamers can be conjugated to a single DNA strand with high yield and efficiency. Functionalized DNA strands can easily be constructed into more compact DNA nanostructures to improve structural stability and cell internalization efficiency. By employing these functionalized DNA nanostructures, cellular DNA-PAINT imaging can be achieved with great precision, super-resolution, multiplexing imaging, and a fast acquisition speed.

Wang et al. exploited single-round immunostaining with DNA-barcoded antibodies to overcome the acquisition speed restrictions.[48] In Figure 3a, the orthogonal DNA docking strands (P) were first conjugated with the distinct targets (T) labeled with corresponding antibodies. Then the imager strands (P*) were sequentially introduced to visualize target signals, followed by the rapid (<10 min) buffer exchange of fluorophore-bearing DNA imager strands. Eight targets in cultured neurons could be distinguished by multiplexed DNA-PAINT, proving a rapid and versatile multiplexed imaging technique for super-resolution imaging of *in situ* cells or tissues.

Most antibodies face size defects to achieve higher efficiency of quantitative DNA-PAINT imaging. Unlike normal antibodies, Affimer reagents have quantitative labeling capabilities and smaller sizes, which are favorable labeling reagents for the docking sites and imager strands. To tackle the limitation of antibody size, Schlichthaerle et al. site-specifically attached an Affimer reagent to a single DNA strand by cysteine−maleimide conjugation and successfully imaged the Affimer-labeled actin network in fixed Cos7 cells with high efficiency via DNA-PAINT imaging (Figure 3b).[49] Subsequently, Sograte-Idrissi et al. used click chemistry reactions to connect the single-stranded DNA with small nanobodies.[50] The nanobodies also were known as small labeling reagents. As shown in Figure 3c, the immunostaining of three different proteins in different organelles with three specific nanobodies such asanti EGFP, mCherry, and mTagBFP allowed them to become fluorescent so that the three corresponding cellular targets could be visualized with 20 nm resolution and within 35 min of acquisition time per target. Recently, Filius et al. proposed that the modification of imager strands also could shorten the acquisition time.[51] The imager strands were loaded into protein Argonaute (Ago). Next, the Ago prearranged the DNA

https://doi.org/10.1021/acsabm.2c00128
ACS Appl. Bio Mater. XXXX, XXX, XXX−XXX

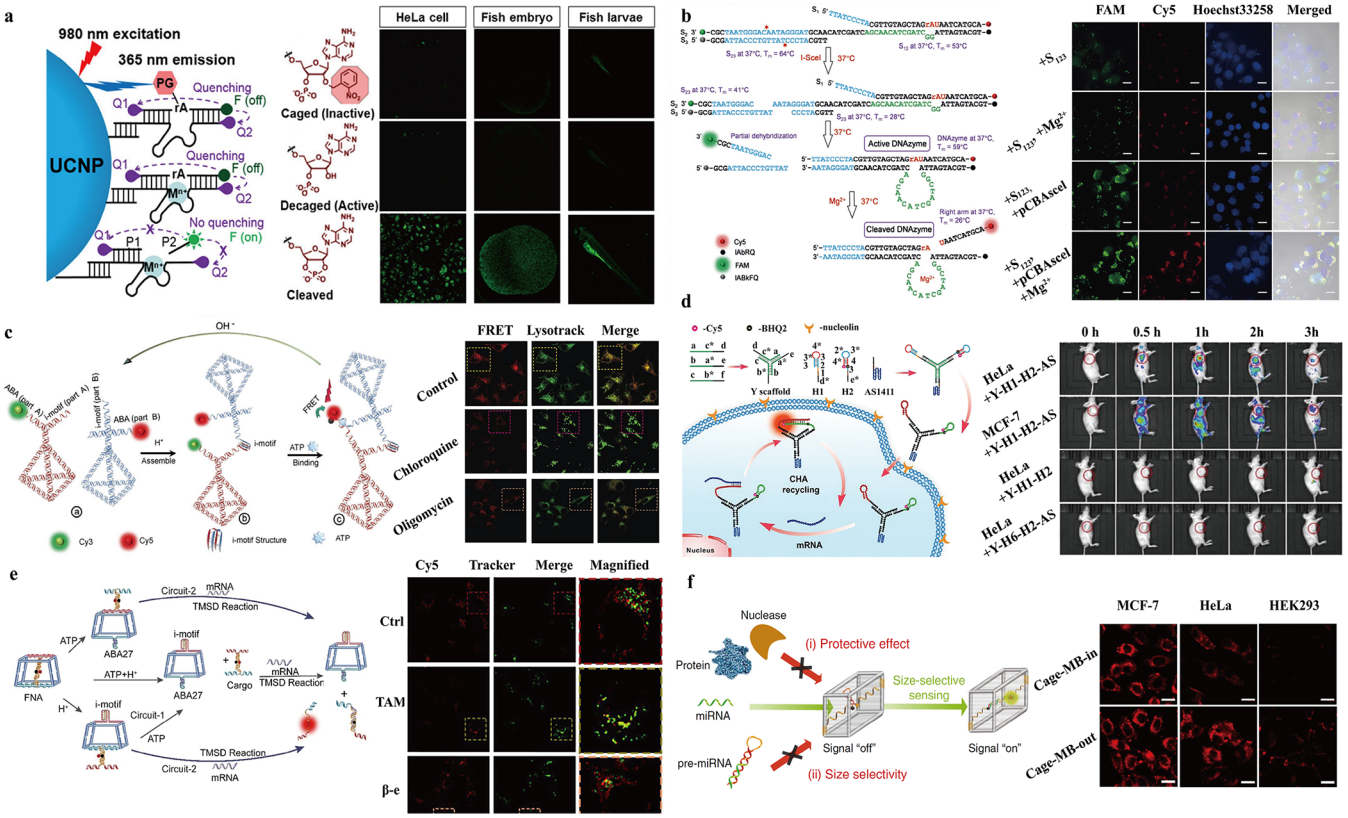

Figure 4. Recent application of DNA nanostructures for intracellular biomolecules imaging. (a) Synthesis of a photocontrollable UCNP and DNAzyme-based nanodevice and its response to Zn^{2+} in early embryos and larvae of zebrafish. Reproduced with permission ref 60. Copyright American Chemical Society 2017. (b) Scheme of I-SceI activation of the DNAzyme for intracellular imaging of Mg^{2+}. Reproduced with permission from ref 61. Copyright Wiley-VCH 2019. (c) Design and characterization of TDNs probe in response to lysosomal acidity and ATP binding in living cells. Reproduced with permission from ref 66. Copyright Wiley-VCH 2019. (d) Mechanism of the aptamer-linked tripartite DNA probe assembly and fluorescence imaging of the surviving mRNA in different tumor-bearing mice with tripartite DNA probes. Reproduced with permission from ref 72. Copyright Royal Society of Chemistry 2020. (e) Illustrating the mechanism of FNA logic circuits and the response to mRNA expression in living cells. Reproduced with permission from ref 74. Copyright Wiley-VCH 2020. (f) Schematic of DNA-based molecular sieve for size-selective molecular imaging in living cells. Reproduced with permission from ref 76. Copyright Springer Nature 2020.

imager strands into a helical conformation, which allowed a faster binding between the imager strand and complementary strand. Furthermore, they compared the Ago-assisted DNA-PAINT (Ago-PAINT) with the general DNA-PAINT method by using a 2D DNA origami structure as the docking site and found that the Ago-assisted method could speed up the acquisition time by an order of magnitude and maintained higher spatial resolution.

Additionally, small and highly specific labeling reagents also help to obtain higher imaging resolution. For example, Strauss et al. employed seven different slow off-rate modified aptamers (SOMAmers, known as tiny DNA nanostructures) to label the docking sites.[52] This work was the first example of using DNA-PAINT imaging in living cells and tracking their membrane targets in their native state. As shown in Figure 3d, the preimmobilization of the living cells was not required with the help of the staining of transmembrane receptor (EGFR) with SOMAmers. More importantly, the average localization precision of SOMAmer-labeled EGFR proteins was about 3.2 nm, and the full-width at half-maximum-limited resolution was less than 8 nm, allowing quantitative sub-10 nm cellular DNA-PAINT imaging. This work also discussed SOMAmers that are specific for GFP-labeled Nup107, suggesting the flexibility of labeling the intracellular targets. Moreover, the genetically encoded self-labeling enzymes can be applied for DNA-PAINT as well. Schlichthaerle et al. presented an approach by using genetically encoded self-labeling enzymes such as SNAP-tag and HaloTag, to achieve higher resolution.[53] They tested BG-modified docking strands targeting SNAP-tags, which were C-terminally fused to NUP96 proteins in U2OS cell lines created by CRISPR/Cas9 engineering. In Figure 3e, the 2D DNA-PAINT images revealed the 8-fold symmetry of NUP96 proteins with super-resolution. They resolved the NUP96 proteins in the Y-complex of the nuclear pore complex with the spacing of only ∼12 nm apart and the single copies of nucleoporins in the human Y-complex in three dimensions with the precision of ∼3 nm. This work provided a high-resolution imaging tool to investigate individual proteins of higher-order protein complexes in cells.

4. OTHER BIOIMAGING EXAMPLES BASED ON DNA NANOSTRUCTURES

Bioimaging plays an important role in the early diagnosis and treatment of diseases. However, the internal, physiological environment is crowded with complex biomolecules and is highly compartmentalized by physiological barriers and membranes. This complexity may lead to the poor performance of synthetic imaging probes in living systems. Imaging probes with high stability, biocompatibility, and low toxicity

https://doi.org/10.1021/acsabm.2c00128
ACS Appl. Bio Mater. XXXX, XXX, XXX−XXX

under physiological conditions need to be fabricated to improve the performance of imaging in living systems.

DNA materials provide a new strategy for bioimaging probe construction. Functionalized DNA nanostructures can be used for biomolecules or cell capture.[54] Scientists successfully assembled several DNA strands into a defined and compact structure to improve its stability. For example, framework nucleic acids (FNA) structures (including a tetrahedron, an octahedron, a DNA triangular prism, and DNA nanotubes) have good biocompatibility, size controllability, and antidegradation ability, all of which can help the structures to maintain their structural integrity in a complex biological environment for several hours and even days.[55] Moreover, combining the DNA materials with inorganic nanoparticles (such as gold nanoparticles, upconversion nanoparticles, and graphene, etc.) could also improve the stability of the DNA materials. In this section, we will focus on the recent advances of other bioimaging methods and targets.

4.1. DNA Nanostructure-Based Intracellular Biomolecules Imaging. The visualization of biomolecules in cells at a nanometer scale led to a greater understanding of how biological processes operated and provided useful information for disease diagnosis. However, only a few biomolecules (metal ions, ATP, RNA, telomerase, and histidine, etc.) were able to achieve sufficiently high resolution for bioimaging applications. DNA nanostructures are competitive candidates serving as imaging agents to tackle this problem due to their specific binding ability for biological targets, outstanding biocompatibility, and stability. DNA nanostructures can be further conjugated with dyes, proteins, and inorganic nanoparticles to achieve diverse features and become a versatile imager, trigger, or carrier for *in vivo* imaging of specific targets that can adapt to different functional imaging modules.

4.1.1. Metal Ion Imaging. In a biological system, metal ions play important roles in stabilizing the conformations of biomolecules and helping catalyze enzymatic reactions. It is crucial to probe the distribution of metal ions because their abnormal distribution can lead to various diseases including neural malfunction, osmolarity imbalance, and cancers. DNAzymes, also known as deoxyribozymes, which catalyze a specific reaction and require metal ions as cofactors, have emerged as a new class of activity-based metal ions imaging agents. The DNAzyme substrate has different melting temperatures before and after the metal-ion-dependent cleavage. The general strategy to construct DNAzymes-based probes is attaching a fluorophore and a quencher to a DNAzyme complex. The cleavage of the DNAzyme structure will release the fluorophore from its quencher to create an "on" fluorescent signal, which allows the imaging of the target metal ions. In 2013, Wu et al. first demonstrated the application of DNAzymes for imaging intracellular metal ions.[56] They conjugated the uranyl-specific 39E DNAzyme with gold nanoparticles, then the DNAzyme would deliver into cultured cells, and the exonuclease-based degradation of DNAzyme ends could be slowed down. The DNAzyme with gold nanoparticles only cleaves the fluorophore-labeled substrate strand in the presence of uranyl, resulting in an increased fluorescence signal and demonstrating the selectivity for imaging of uranyl inside live cells. After this work, a set of DNAzymes-based imaging probes has been reported for the cellular imaging of Na^+,[57] Cu^{2+},[58] and Pb^{2+}.[59]

Recently, Yang et al. reported a Zn^{2+}-specific near-infrared (NIR) DNAzyme nanoprobe for real-time metal ion tracking in early embryos and the larvae of zebrafish.[60] In Figure 4a, they functionalized the UCNP of a photocaged DNAzyme by attaching a fluorophore (F) and two quenchers (Q1, Q2) to the UCNP. The UCNP generated fluorescence emission at 365 nm wavelength and removed the protection of the 2′-nitrobenzyl photocage group (PG) for the ribonucleotide adenosine (rA) site under 980 nm laser irradiation. Then the restored 2′-OH of adenosine ribonucleotide assisted in the Zn^{2+} specific cleavage of the single substrate strand, leading to an "on" fluorescence signal due to the fluorophore dissociating from the enzyme strand. This study achieved spatial and temporal optical control of the DNAzyme-UCNP system for higher penetration depth metal ions detection *in vivo*.

More recently, Lin et al. introduced an approach of using homing endonuclease (I-SceI) to activate the DNAzyme for the fluorescent imaging of Mg^{2+} in living cells.[61] As shown in Figure 4b, the bioorthogonal method for activating the DNAzyme catalytic ability is carried out by conjugating the I-SceI enzyme recognition site with the DNAzyme binding arms. When the cell expressed I-SceI, the recognition site cleaved and converted the DNAzyme into its active conformation, enabling it to catalyze the cleavage of the substrate strand in the presence of Mg^{2+}. Then a fluorescent signal was detected from the releasing of the strand containing the fluorophore. The endogenous and bioorthogonal control of a DNAzyme led to its specific binding to Mg^{2+}, which made it important for the understanding of the distribution and fluctuation of Mg^{2+} in living cells. Using DNAzyme-based probes for detection of other metal ions has also been reported such as K^+, Ag^+, Hg^{2+}, and Co^{2+}.[62] Since metal ions are related to many diseases, these works help researchers understand the roles of metal ions in many physiological processes.

4.1.2. ATP Imaging. The characterization of ATP dynamics is essential for exploring the processes that range from neurotransmission to the chemotaxis of immune cells. Researchers found that DNA aptamer-based probes can be applied for ATP imaging in live cells.[63] These self-assembled DNA probes possessed excellent cell membrane permeability and biocompatibility. For example, Zheng et al. designed an ATP aptamer-based DNA probe for ATP imaging in living cells.[64] They anchored two split ATP aptamers labeled with donor and acceptor fluorophores on a DNA triangular prism. In the presence of ATP, two aptamer strands were brought closer and generated a FRET signal, thus enabling the intracellular ATP imaging. Moreover, the DNA triangular prism provided the reasonable protection of the split aptamer from nuclease degradation. Using the split aptamer with "off−on" mechanism of FRET could efficiently avoid false-positive signals.

Structure-switching aptamers were also involved in DNA bioimaging probe design. Zhao et al. reported a luminescence-activatable DNA nanodevice probe composed of DNA aptamer and UCNP to detect ATP in a living system.[65] The aptamer strand modified with a fluorophore Cy3 was initially locked by a complementary DNA strand conjugated with a quencher strand and a photocleavable (PC) group, providing a low fluorescence background and preventing its ATP binding activity. Upon UV light irradiation, the complementary DNA strand split into two short strands due to the photolysis of the PC group. The aptamer switched its structure to bind ATP, resulting in the dissociation of the quencher strand and the significant increase of the fluorescent signal for ATP imaging. This approach provided a general method for the NIR-

https://doi.org/10.1021/acsabm.2c00128
ACS Appl. Bio Mater. XXXX, XXX, XXX−XXX

controlled imaging of various targets by incorporating different aptamers with UCNP.

More recently, Peng et al. designed an aptamer functionalized FNA nanoplatform that could be dynamically manipulated in living cells for subcellular ATP imaging. The nanoplatform was constructed by two DNA tetrahedrons (TDNs) with different branched vertexes. As depicted in Figure 4c, both of the tetrahedrons carried a bimolecular i-motif and a split ATP aptamer.[66] The TDNs were assembled into heterodimeric architectures in the lysosomes of living cells due to their acidic environment and in response to endogenous ATP binding. This dimerization process was reversible so that it could be dynamically manipulated by adjusting intracellular pH and ATP levels with external drug stimuli. By monitoring the structural conformation change, the subcellular ATP could be visualized efficiently.

4.1.3. RNA Imaging. RNA molecules play various significant biological roles such as coding, decoding, regulation, and expression of genes. Monitoring the distribution of RNA in a living system is crucial for understanding the biological functions of RNA and identifying RNA-related diseases. However, it is difficult to image cellular RNA due to its low expression level in cells. To tackle this problem, researchers integrated several signal amplification methods (e.g., hybridization chain reaction (HCR),[67] catalyzed hairpin assembly (CHA),[68] fuel stimulant-powered amplification (FSP),[69] and DNAzyme motor-powered amplification (DMP)[70]) with DNA devices. Inspired by these amplification methods, many novel DNA probes for RNA imaging have been developed. For example, He et al. reported an entropy-driven 3D DNA amplifier (EDTD) for the specific mRNA target imaging based on a CHA strategy.[71] The EDTD amplifier was anchored on a DNA tetrahedral framework to exhibit significantly enhanced biostability and cellular delivery efficiency. With the help of an entropy-driven force, an autonomous DNA circuit was initiated by the mRNA target/EDTD interaction and achieved significant signal amplification for the target mRNA imaging. Recently, Wu et al. reported a DNA probe using the CHA circuit strategy for the detection of the target mRNA that was in low abundance in cells and mice.[72] In this work, a Y-shaped DNA nanostructure was hybridized with both phosphorothioated substrate hairpins and an AS1411 aptamer to fabricate a DNA probe (Figure 4d). The DNA probe could recognize the small amount of the target mRNA with good fluorescence signal *in vivo*, showing great potential for early stage clinical diagnosis and treatment under the guidance of fluorescence imaging. Similarly, Liu et al. demonstrated another Y-shaped DNA nanodevice, which could perform intracellular nonenzymatic *in situ* growth of 3D DNA nanospheres to detect mRNAs or proteins in living cells.[73] The locked triggering probe would open in the presence of target mRNA, leading to a fluorescence signal and marking the intracellular position of the target. Then, mediated by the sequential assembly of the Y-shaped structure, the opened triggering hairpin probes activated the gradual growth of spherical structures to obtain images with different fluorescence signal. Finally, these fluorescence images were merged, and it was demonstrated that the target and self-assembled spherical structures were in the same location. As a result, this Y-shaped DNA nanodevice successfully achieved the real-time *in situ* imaging of intracellular mRNA.

Researchers also introduced logic circuits into DNA nanostructures to achieve high-precision RNA imaging. For instance, Wang et al. created two logic circuits, OR-AND and AND-AND cascades, to improve the accuracy of subcellular mRNA imaging (Figure 4e).[74] They constructed a logical control DNA nanodevice by embedding the i-motif structure and ATP aptamers in a truncated square pyramid cage. Then the assembled nanodevice would release the sensing element and achieve the target mRNA imaging in response to the intracellular H^+ and ATP.

Additionally, an enzyme-propelled RNA walker can be applied for amplifying biorecognition signals of microRNA (miRNA) imaging. For example, Xiao et al. constructed a nanomachine with amplified fluorescence signal outputs for cellular miRNA imaging. They first wrapped a single wall carbon nanotube (SWCNT) with a fluorophore (6-FAM) labeled DNA diblock oligomers.[75] Then the RNA walker (single-stranded RNA) complementary to DNA oligomers would form DNA/RNA heteroduplexes. In the presence of duplex-specific nuclease (DSN), the selective digestion of DNA in heteroduplexes released the FAM-labeled DNA and led to fluorescence diminishing of the target SWCNT. The released RNA walker would subsequently bind to another DNA strand on the SWCNT and initiate the next cleavage cycle, thus amplifying signal outputs achieved by high target recycling kinetics. Finally, the nanomachine complementary to miRNA and DSN could be delivered to HeLa cells to detect the cellular miRNA effectively.

Recently, Fu et al. reported a DNA-based molecular sieve for size-selective molecular recognition in living cells.[76] As shown in Figure 4f, they encapsulated different functional nucleic acid probes (e.g., DNAzymes, aptamers, and molecular beacons) into the inner cavity of cavity-tunable DNA nanocages. Because of the size limitation, only the small target molecules could enter the cavity for efficient molecular recognition, whereas large molecules were prohibited. Furthermore, the DNA nanocages exhibited enhanced anti-interference ability against nuclease degradation and nonspecific protein binding. They also found that the DNA molecular sieve could selectively recognize the mature microRNA by fluorescence imaging in living cells.

4.1.4. Other Biomolecules Imaging. Despite imaging cellular metal ions, ATP, and RNA, the imaging of cellular proteins and amino acids has also attracted broad attention. In most intracellular reactions, proteins and amino acids act as the reactive agents or catalysts, which play a vital role in maintaining the cell's homeostasis. Although only a tiny amount of them are inside the cell, a small change of the content may be related to, or even cause, some diseases. Thus, capturing the small changes can help us find more solutions for disease diagnose or therapies, requiring the development of an ultrasensitive imaging probe, telomerase and histidine are among the most popularly studied.

The length of telomeres in healthy cells undergoes progressive shortening during cell proliferation but they maintain the original length in most cancer cells by telomerase.[77] Therefore, telomerase is a promising biomarker for early cancer diagnosis and tumor progression monitoring. In an early study, Pavlov et al. exploited the hemin/G-quadruplex HRP-mimicking DNAzyme for chemiluminescent detection of telomerase.[78] This method only detected telomerase extracted from HeLa cells. And the chemiluminescence intensity correlated to the telomerase content. Note that this imaging probe only applied to *in vitro* assays, which cannot provide information on telomerase activities in living

https://doi.org/10.1021/acsabm.2c00128
ACS Appl. Bio Mater. XXXX, XXX, XXX−XXX

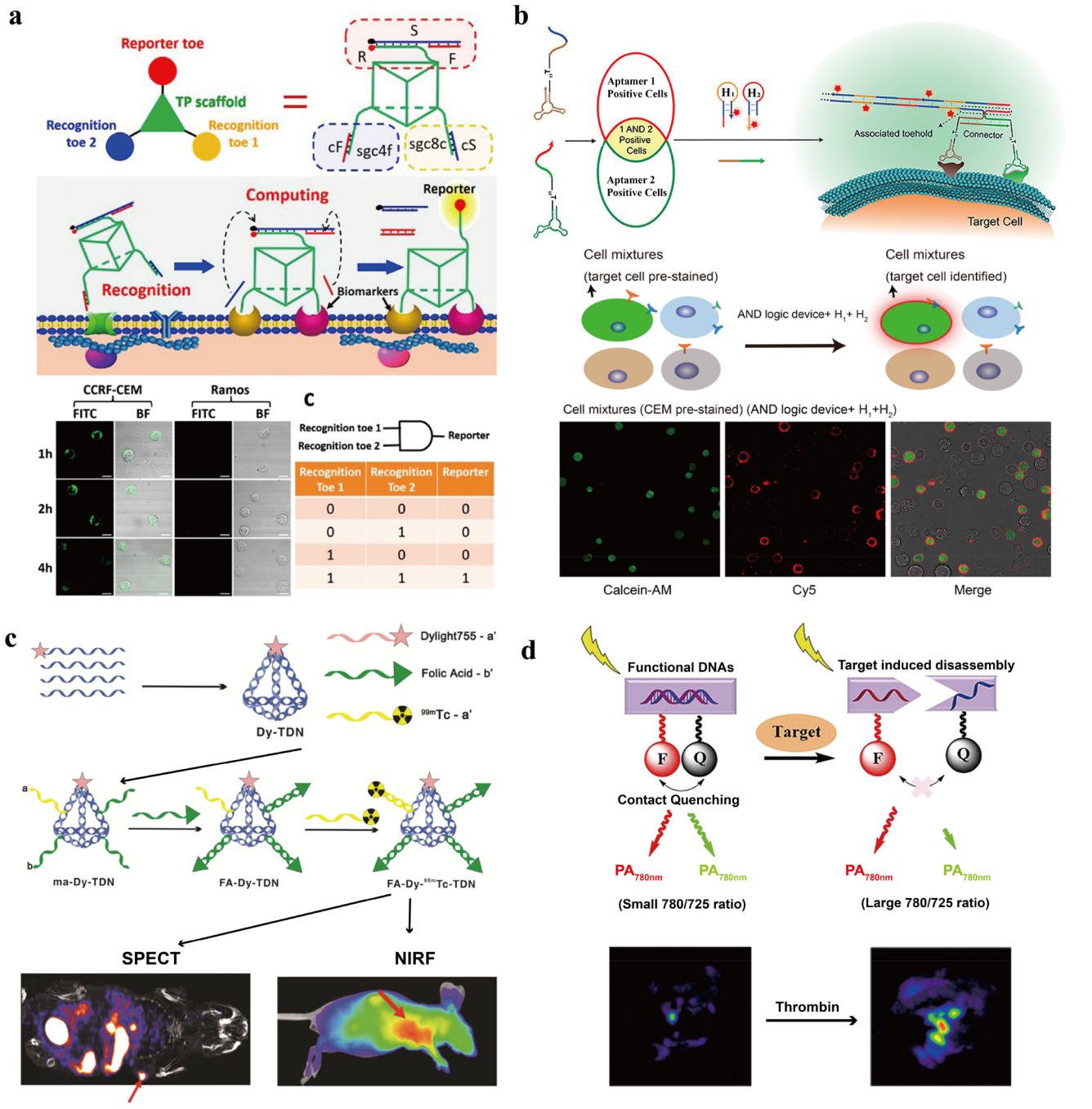

Figure 5. Imaging of biomarkers on cell membrane. (a) DNA triangular prism-based logic gate nanomachine mechanism for imaging the overexpressed cancer cell biomarkers with bispecific recognition sites. Reproduced from ref 93. Copyright American Chemical Society 2018. (b) Design and mechanism for dual-aptamer-based AND logic device for cell identification and isolation. Reproduced from ref 95. Copyright American Chemical Society 2019. (c) Design of dual-modality imaging probe based on double helix DNA tetrahedron for SPECT and NIRF imaging *in vivo*. Reproduced from ref 88. Copyright American Chemical Society 2016. (d) Aptamer-based activatable PA probe for ratiometric PA imaging of target molecule in living mice. Reproduced from ref 92. Copyright American Chemical Society 2017.

systems. Later on, amplification methods with high sensitivity for telomerase detection were developed such as polymerase chain reaction (PCR)-based classic telomeric repeat amplification protocols[79] and isothermal DNA amplification.[80] However, they are still limited to working with cell extracts. To realize the amplified detection of telomerase in living cells, Fan et al. introduced a cascade amplification reaction-based (CAR) nanoprobe for intracellular telomerase detection by incorporating MnO_2 nanosheets with DNAzyme and catalytic hairpin assembly.[77] A large amount of Mn^{2+} ions generated from MnO_2 nanosheets degradation can activate DNAzyme as a metal cofactor and cleave the telomere sequence (T strand) from DNAzyme strand. The released T strands hybridize to H1 and further trigger the binding to H2, which results in the fluorescence recovering from the H2 strand. This cascade amplification process achieved a higher fluorescence signal output and enabled the ultrasensitive imaging of telomerase in living cells. Following that, Guo et al. reported a surface-enhanced Raman scattering-based DNA tetrahedron probe for the simultaneous *in situ* detection of intracellular telomerase.[81]

https://doi.org/10.1021/acsabm.2c00128
ACS Appl. Bio Mater. XXXX, XXX, XXX−XXX

This probe showed excellent specificity and sensitivity in the detection of telomerase, with LODs of 7.6 × 10−16 IU, enabling the distinction between normal cells and cancer cells. These new developments facilitated researchers in understanding the pathogenesis for clinical therapy.

L-Histidine (L-His) is an essential amino acid that cannot be synthesized *de novo* in humans but plays an vital role for human growth, metal transmission, neurotransmission, and neuromodulation.[82] An abnormal level of histidine or histidine-rich proteins often corresponds to disease development. Therefore, selective and sensitive detection of histidine in urine or living cells has become significant and indispensable. *In vitro* selection of RNA-cleaving DNAzymes (RCDs) found that the L-His-dependent RCDs have excellent specificity and sensitivity of L-His, which brings new insight for L-His detection.[83] For example, Kong et al. developed a DNAzyme-based sensing platform using an endonuclease-based enzymatic recycling cleavage strategy for L-His detection.[84] This enzymatic signal amplification strategy affords high sensitivity, resulting in a detection limit of 200 nM for L-His. Moreover, Meng et al. proposed a DNA dendrimer nanocarrier with histidine-dependent DNAzyme for intracellular L-His and ATP detection.[85] This nanocarrier successfully self-delivered into living cells with no change in sensitivity or specificity and recognized the histidine and ATP efficiently. To amplify the signal output, He et al. reported an HCR-based DNAzyme fluorescent sensor to detect L-His associated with urine samples.[86] Here, L-His was a trigger to initiate the cleavage of DNAzyme substrate strands; the released substrates were primers to trigger a cascade of hybridization events. The HCR amplified the oligonucleotide products, allowing more G-quadruplex structures to bind with porphyrin molecules and enhance its fluorescent intensity as efficient signal output. Recently, Xu et al. fabricated an electrochemical nanotool on the basis of rational integration between a nanopipette and synthetic DNAzyme for quantification of amino acids in a single cell, which is exemplified by L-His.[87] Ionic current rectification response will be efficiently generated upon L-His-provoked cleavage of the DNA molecules. This work demonstrated that synthetic DNAzyme facilitating electrochemistry quantification could provide a new way for identifying amino acids in living cells.

4.2. DNA Nanostructures for Imaging Cell Membrane Biomarkers. DNA nanostructure-based imaging agents were widely used for the selective recognition of cell membrane biomarkers. The small DNA structures could be conjugated with other DNA nanostructures or inorganic nanoparticles to achieve high targeting ability, stability, cellular internalization, and versatile functionalities that adapt to different imaging modules. The DNA nanostructure-based materials have been proven to be the specific targeting imaging agents for different imaging modules *in vivo* including near-infrared fluorescent imaging (NIRF),[88] PET,[89] MRI,[90] CT,[91] SPECT,[88] and photoacoustic imaging (PA).[92]

4.2.1. Logic Gates Assisted Selective Recognition of Target Cancer Cells In Vitro. The precise recognition of target tumor cells among large amounts of normal cells is still challenging. Researchers have developed a series of aptamer logic gate-based DNA nanodevices for the recognition of target cancer cells. For instance, Peng et al. designed a 3D triangular prism (TP) DNA structure as a logic gate (AND gate) to identify bispecific biomarkers.[93] They selected two aptamers, sgc8c and sgc4f, as recognition molecules targeting overexpressed biomarkers in CEM cells. Moreover, the Ramos cell membranes under-expressed these biomarkers, thus making it easy to be distinguished from others. As shown in Figure 5a, f5 the TP nanodevice performed a strand displacement reaction and recombination to turn on the fluorescence signal in the presence of both biomarkers on the same cell only. The change in the fluorescence signal could be observed by fluorescence spectroscopy imaging, flow cytometry, and confocal imaging, thereby enabling the rapid analysis of specific cancer cells. Furthermore, the accuracy of cell identification was significantly improved by this TP nanodevice compared to linear double strand DNA-based circuits. The TP nanodevice was easily incorporated with all logic units into one triangular scaffold. Similarly, Zhou et al. designed a switchable DNA tetrahedral nanostructure[94] with AND logic gates for cancer cells recognition. The presence of K^+ helped to stabilize the formation of G-quadruplexes or T−A•T triplexes between each monomer DNA tetrahedra structure, thus leading to dimer or trimer formation. In contrast, the crown ether or pH conditions separated the dimer/trimer tetrahedral nanostructures. Then they designed selective dimer structures using miRNA so that the dimer structures only formed in the presence of the target miRNA, enabling the specific imaging of cancer cells.

Recently, Chang et al. employed multiple DNA aptamers to identify cancer biomarkers based on activation signal integration and amplification.[95] They demonstrated an AND Boolean logic operation analyzing multiple biomarkers and precisely labeling the targeted cell subtype with the coexistence of large populations of similar cells. As shown in Figure 5b, the logic device consisted of three active elements: the single stranded DNA detector (aptamer-spacer-toehold [Apt-S-T]) to reduce steric hindrance of structures, the ssDNA connector to hybridize with different Apt-S-T detectors, and the H1 and H2 hairpin probes to generate HCR amplification. In this work, the double aptamer AND logic device achieved single-step identification and isolation of cancer cells with enhanced sensitivity and accuracy.

4.2.2. DNA-Based Imaging Modulars for Biomarker Recognition In Vivo. Radionuclide-based imaging techniques such as SPECT and PET are more widely used imaging modalities in clinics than other molecular imaging techniques due to their great tissue penetration and quantitative analysis ability. Radioisotopes, such as ^{125}I, ^{99}Tc, and ^{18}F, coupled with DNA aptamers were able to function as highly specific and sensitive radiopharmaceuticals. However, the SPECT and PET required hazardous ionizing radiation and a time-consuming image reconstruction process. Therefore, there are urgent needs for the development of nonionizing radiation-based real-time imaging methods.

Among different imaging methods, FL is the most adapted imaging module due to its low cost and high sensitivity and has been interacted with DNA nanostructures. Jiang et al. proposed a multiple-armed duplex DNA tetrahedron probe that could specifically bind with folate receptor-positive tumor cells.[88] They first assembled the duplex DNA tetrahedron structures with different protruding strands at each arm chains (Figure 5c). Then they modified the tagged single-strand DNA with NIR fluorescent dye Dylight-755, radioactive isotope label ^{99m}Tc, or folic acid to complement the protruding strands on different arm chains, thereby enabling the target tumor imaging with both NIRF and SPECT modalities. The results showed

https://doi.org/10.1021/acsabm.2c00128
ACS Appl. Bio Mater. XXXX, XXX, XXX−XXX

that this probe had good stability and could keep integrity in 80% mouse serum at 37 °C for 12 h.

In addition to fluorescence imaging, MRI and CT are known as anatomical imaging modalities for clinics imaging with high resolution and a spatial penetration depth. Using aptamers as targeting components, these modalities can be used for biomarkers or tumor imaging *in vivo*. For example, aptamer-based MRI contrast agents are generally designed by combining an aptamer with superparamagnetic iron oxides. Zhao et al. reported a DNA-Mn hybrid nanoflower (DMNF) for tumor site-activated MR imaging,[96] in which the manganese ions mediated enzymatic biomineralization of DNA nanoflowers. The target probe was synthesized by using a long DNA strand as a template via nucleation and growth of Mn2PPi. Then the DNA template was encoded with a DNA aptamer sequence to achieve enhanced cellular uptake and tumor targeting, while the paramagnetic Mn^{2+} was explored as the cofactor of a DNA polymerase for the extension of the long DNA strand. Because of the acidic environment of tumor sites, the DMNF showed morphology collapse and Mn^{2+} release, resulting in an enhanced T_1-weighted MRI effect for the MR imaging of DMNF-treated tumor sites.

Recently, PA imaging with higher penetration depth and excellent spatial resolution has emerged as an alternative method to MRI. Unlike PET and SPECT that suffer from hazardous ionizing radiation and limited spatial resolution, PA imaging is a safer, real-time, and noninvasive imaging method. Aptamer-based PA probes have been investigated for specific targets imaging *in vivo*. For instance, Zhang et al. proposed thrombin activatable DNA aptamer-based PA probes for *in vivo* imaging.[92] As shown in Figure 5d, the sensing system was based on the contact quenching between the DNA strands conjugated with a NIR dye (IRDye 800CW) and its dark quencher (IRDye QC-1), which was mediated by DNA aptamer through the duplex formation. The thrombin-induced disassembly of the DNA complex would inhibit the contact quenching process and increase the PA signal ratio at 780/725 nm. Therefore, the quantitative analysis of the change of PA signal enabled the selective imaging of the aptamer recognized thrombin. In addition, Kim et al. reported that DNA aptamer conjugated with gold nanoparticles were suitable for PA imaging of human matrix metalloproteinase-9 (hMMP-9) *in vivo*.[97] The modification of DNA aptamers enabled sensitive and selective detection of hMMP-9. The gold nanoparticles core enhanced the optical absorption to the first NIR window and made it suitable for PA imaging. All of these examples suggest that DNA aptamers, combined with inorganic nanoparticles, can enhance the targeting ability of probes for application *in vivo*.

5. CONCLUSION AND OUTLOOK

DNA nanostructures have been demonstrated as great nanoconstruction material and have shown great potential in biomedical applications. Studies have demonstrated that self-assembled DNA nanodevices have higher cellular uptake rate and greater resistance to nuclease degradation compared to unassembled DNA.[98] The modification of DNA nanostructures allowed these materials to achieve high biocompatibility, good robustness, competent responsiveness, and improved cell permeability. This review summarized the recent applications of self-assembled DNA nanostructures for bioimaging applications. We focused on DNA-PAINT imaging and modification methods of the DNA nanodevice probe. Additionally, DNA nanoprobes for *in vivo* imaging were also discussed. Despite these great achievements, there are several remaining challenges, as well as opportunities, in DNA nanostructure-based bioimaging.

The DNA-PAINT imaging technique has achieved tremendous advances such as in multiplexing, minute level acquisition speed, and molecular level resolution in fixed cells. DNA-PAINT technique for live cell imaging enables the ability to locate dynamic features of intracellular proteins, visualize protein interactions with super-resolution, and quantify the concentrations of cellular biomolecules. However, the resolution of DNA-PAINT imaging in living cells is not as high as that in fixed cells because the living cells have a more complex, sensitive, and dynamic environment. Moreover, high-resolution living cells imaging is influenced by the stability of DNA materials, potential incorrect interactions between DNA with cellular nucleic acids or proteins, and targets labeling in different living cells. These advances and challenges have opened new opportunities for future research in DNA-PAINT imaging for living cells. For example, the acquisition speed needs to be further improved to capture the fast and weak motions of living cells. In addition, research efforts are needed on decreasing the nonspecific interactions between DNA material-based probes and cellular nucleic acids. Finally, it will be helpful to introduce new functionalities by exploring novel assembly methods and modification strategies of DNA nanostructures.

DNA nanostructures, including DNAzyme, DNA aptamers, and FNA, have been incorporated with small molecules, proteins, or nanoparticles to fabricate different functional imaging probes. For example, aptamers have been used to differentiate disease-specific targets in cancer cell research. In addition, aptamer-based probes have shown great promise for targeted cancer diagnostics in a preclinical study. DNA nanostructures brought exciting features and allowed new constructions such as multimodal imaging modalities. As described in section 4, the DNA tetrahedron probes have taken advantage of the qualitative imaging of NIRF and the high sensitivity and excellent detecting depth of SPECT. This DNA tetrahedron served as a NIRF and SPECT dual-modality tumor target imaging probe, which offered images of the target tumor with high resolutions and penetration depths. Although DNA nanostructures have many advantages, applying DNA nanostructures in physiological environments still has challenges including limited stability in biological media, poor cell uptake efficiency, and various immune responses. For example, most DNA nanostructures need a certain Mg^{2+} concentration to maintain the integrity of the designed structure. However, physiological environments with lower Mg^{2+} concentrations and the presence of nucleases will quickly degrade the DNA nanostructures. Therefore, more external enzymatic and chemical modification methods need to be explored in the future to fix these issues. More exciting functionalities and applications are expected to benefit future bioimaging studies for disease diagnostics.

In conclusion, the DNA nanostructures-based probes for bioimaging are undergoing fast development. Many reliable and practical modification methods have been validated to improve their properties. These functionalized DNA nanostructures probes enable fast detection of various targets in the molecular and cellular level. Future developments in self-

https://doi.org/10.1021/acsabm.2c00128
ACS Appl. Bio Mater. XXXX, XXX, XXX−XXX

assembled DNA nanostructures offer unprecedented opportunities for bioimaging.

AUTHOR INFORMATION

Corresponding Author

Fei Zhang − *Department of Chemistry, Rutgers University, Newark, New Jersey 07102, United States*; orcid.org/0000-0002-3177-7547; Phone: 973-353-5520; Email: fei.zhang@rugers.edu

Authors

Qi Yang − *Department of Chemistry, Rutgers University, Newark, New Jersey 07102, United States*

Xu Chang − *Department of Chemistry, Rutgers University, Newark, New Jersey 07102, United States*

Jung Yeon Lee − *Department of Chemistry, Rutgers University, Newark, New Jersey 07102, United States*

Tiffany Olivera − *Department of Chemistry, Rutgers University, Newark, New Jersey 07102, United States*

Minu Saji − *Department of Chemistry, Rutgers University, Newark, New Jersey 07102, United States*

Henry Wisniewski − *Department of Chemistry, Rutgers University, Newark, New Jersey 07102, United States*

Suchan Kim − *Department of Chemistry, Rutgers University, Newark, New Jersey 07102, United States*

Complete contact information is available at: https://pubs.acs.org/10.1021/acsabm.2c00128

Notes

The authors declare no competing financial interest.

ACKNOWLEDGMENTS

This work is supported by a US National Science Foundation (NSF) Faculty Early Career Development Award (DMR-2046835), an NSF grant (CCF-2007821), a Busch Biomedical Grant, and a faculty Startup Fund from Rutgers University.

REFERENCES

(1) Yan, X.; Huang, S.; Wang, Y.; Tang, Y.; Tian, Y. Bottom-Up Self-Assembly Based on DNA Nanotechnology. *Nanomaterials* **2020**, *10* (10), 2047.

(2) Li, F.; Li, J.; Dong, B.; Wang, F.; Fan, C.; Zuo, X. DNA nanotechnology-empowered nanoscopic imaging of biomolecules. *Chem. Soc. Rev.* **2021**, *50* (9), 5650−5667.

(3) Zeng, Y.; Nixon, R. L.; Liu, W.; Wang, R. The applications of functionalized DNA nanostructures in bioimaging and cancer therapy. *Biomaterials* **2021**, *268*, 120560.

(4) Seeman, N. C. Nucleic acid junctions and lattices. *J. Theor. Biol.* **1982**, *99* (2), 237−247.

(5) Chen, J.; Seeman, N. C. Synthesis from DNA of a molecule with the connectivity of a cube. *Nature* **1991**, *350* (6319), 631−633.

(6) Fu, T. J.; Seeman, N. C. DNA double-crossover molecules. *Biochemistry* **1993**, *32* (13), 3211−3220.

(7) Winfree, E.; Liu, F.; Wenzler, L. A.; Seeman, N. C. Design and self-assembly of two-dimensional DNA crystals. *Nature* **1998**, *394* (6693), 539−544.

(8) Yan, H.; Park, S. H.; Finkelstein, G.; Reif, J. H.; LaBean, T. H. DNA-Templated Self-Assembly of Protein Arrays and Highly Conductive Nanowires. *science* **2003**, *301* (5641), 1882−1883.

(9) He, Y.; Ye, T.; Su, M.; Zhang, C.; Ribbe, A. E.; Jiang, W.; Mao, C. Hierarchical self-assembly of DNA into symmetric supramolecular polyhedra. *Nature* **2008**, *452* (7184), 198−201.

(10) Carter, J. D.; Labean, T. H. Organization of Inorganic Nanomaterials via Programmable DNA Self-Assembly and Peptide Molecular Recognition. *ACS Nano* **2011**, *5* (3), 2200−2205.

(11) Zheng, J.; Birktoft, J. J.; Chen, Y.; Wang, T.; Sha, R.; Constantinou, P. E.; Ginell, S. L.; Mao, C.; Seeman, N. C. From molecular to macroscopic via the rational design of a self-assembled 3D DNA crystal. *Nature* **2009**, *461* (7260), 74−77.

(12) Goodman, R. P.; Berry, R. M.; Turberfield, A. J. The single-step synthesis of a DNA tetrahedron. *Chem. Commun.* **2004**, No. 12, 1372.

(13) Shih, W. M.; Quispe, J. D.; Joyce, G. F. A 1.7-kilobase single-stranded DNA that folds into a nanoscale octahedron. *Nature* **2004**, *427* (6975), 618−621.

(14) Wei, B.; Dai, M.; Yin, P. Complex shapes self-assembled from single-stranded DNA tiles. *Nature* **2012**, *485* (7400), 623−626.

(15) Ke, Y.; Ong, L. L.; Shih, W. M.; Yin, P. Three-Dimensional Structures Self-Assembled from DNA Bricks. *Science* **2012**, *338* (6111), 1177−1183.

(16) Ong, L. L.; Hanikel, N.; Yaghi, O. K.; Grun, C.; Strauss, M. T.; Bron, P.; Lai-Kee-Him, J.; Schueder, F.; Wang, B.; Wang, P.; Kishi, J. Y.; Myhrvold, C.; Zhu, A.; Jungmann, R.; Bellot, G.; Ke, Y.; Yin, P. Programmable self-assembly of three-dimensional nanostructures from 10,000 unique components. *Nature* **2017**, *552* (7683), 72−77.

(17) Rothemund, P. W. K. Folding DNA to create nanoscale shapes and patterns. *Nature* **2006**, *440* (7082), 297−302.

(18) Andersen, E. S.; Dong, M.; Nielsen, M. M.; Jahn, K.; Subramani, R.; Mamdouh, W.; Golas, M. M.; Sander, B.; Stark, H.; Oliveira, C. L. P.; Pedersen, J. S.; Birkedal, V.; Besenbacher, F.; Gothelf, K. V.; Kjems, J. Self-assembly of a nanoscale DNA box with a controllable lid. *Nature* **2009**, *459* (7243), 73−76.

(19) Douglas, S. M.; Dietz, H.; Liedl, T.; Hogberg, B.; Graf, F.; Shih, W. M. Self-assembly of DNA into nanoscale three-dimensional shapes. *Nature* **2009**, *459* (7245), 414−418.

(20) Douglas, S. M.; Marblestone, A. H.; Teerapittayanon, S.; Vazquez, A.; Church, G. M.; Shih, W. M. Rapid prototyping of 3D DNA-origami shapes with caDNAno. *Nucleic Acids Res.* **2009**, *37* (15), 5001−5006.

(21) Dietz, H.; Douglas, S. M.; Shih, W. M. Folding DNA into Twisted and Curved Nanoscale Shapes. *Science* **2009**, *325* (5941), 725−730.

(22) Zhang, F.; Jiang, S.; Wu, S.; Li, Y.; Mao, C.; Liu, Y.; Yan, H. Complex wireframe DNA origami nanostructures with multi-arm junction vertices. *Nat. Nanotechnol.* **2015**, *10* (9), 779−784.

(23) Benson, E.; Mohammed, A.; Gardell, J.; Masich, S.; Czeizler, E.; Orponen, P.; Högberg, B. DNA rendering of polyhedral meshes at the nanoscale. *Nature* **2015**, *523* (7561), 441−444.

(24) Han, D.; Qi, X.; Myhrvold, C.; Wang, B.; Dai, M.; Jiang, S.; Bates, M.; Liu, Y.; An, B.; Zhang, F.; Yan, H.; Yin, P. Single-stranded DNA and RNA origami. *Science* **2017**, *358* (6369) DOI: 10.1126/science.aao2648.

(25) Liu, W.; Zhong, H.; Wang, R.; Seeman, N. C. Crystalline Two-Dimensional DNA-Origami Arrays. *Angew. Chem., Int. Ed.* **2011**, *50* (1), 264−267.

(26) Iinuma, R.; Ke, Y.; Jungmann, R.; Schlichthaerle, T.; Woehrstein, J. B.; Yin, P. Polyhedra Self-Assembled from DNA Tripods and Characterized with 3D DNA-PAINT. *Science* **2014**, *344*, 65−69.

(27) Tikhomirov, G.; Petersen, P.; Qian, L. Fractal assembly of micrometre-scale DNA origami arrays with arbitrary patterns. *Nature* **2017**, *552* (7683), 67−71.

(28) Yao, G.; Zhang, F.; Wang, F.; Peng, T.; Liu, H.; Poppleton, E.; Šulc, P.; Jiang, S.; Liu, L.; Gong, C.; Jing, X.; Liu, X.; Wang, L.; Liu, Y.; Fan, C.; Yan, H. Meta-DNA structures. *Nat. Chem.* **2020**, *12* (11), 1067−1075.

(29) Tian, Y.; Lhermitte, J. R.; Bai, L.; Vo, T.; Xin, H. L.; Li, H.; Li, R.; Fukuto, M.; Yager, K. G.; Kahn, J. S.; Xiong, Y.; Minevich, B.; Kumar, S. K.; Gang, O. Ordered three-dimensional nanomaterials using DNA-prescribed and valence-controlled material voxels. *Nat. Mater.* **2020**, *19* (7), 789−796.

(30) Woo, S.; Rothemund, P. W. K. Programmable molecular recognition based on the geometry of DNA nanostructures. *Nat. Chem.* **2011**, *3* (8), 620−627.

(31) Gerling, T.; Wagenbauer, K. F.; Neuner, A. M.; Dietz, H. Dynamic DNA devices and assemblies formed by shape-complementary, non-base pairing 3D components. *science* **2015**, *347* (6229), 1446−1452.
(32) Cox, W. G.; Singer, V. L. Fluorescent DNA hybridization probe preparation using amine modification and reactive dye coupling. *BioTechniques* **2004**, *36* (1), 114−122.
(33) Schröder, T.; Scheible, M. B.; Steiner, F.; Vogelsang, J.; Tinnefeld, P. Interchromophoric Interactions Determine the Maximum Brightness Density in DNA Origami Structures. *Nano Lett.* **2019**, *19* (2), 1275−1281.
(34) Praetorius, F.; Dietz, H. Self-assembly of genetically encoded DNA-protein hybrid nanoscale shapes. *Science* **2017**, *355* (6331), No. eaam5488.
(35) Li, S.; Jiang, Q.; Liu, S.; Zhang, Y.; Tian, Y.; Song, C.; Wang, J.; Zou, Y.; Anderson, G. J.; Han, J.-Y.; Chang, Y.; Liu, Y.; Zhang, C.; Chen, L.; Zhou, G.; Nie, G.; Yan, H.; Ding, B.; Zhao, Y. A DNA nanorobot functions as a cancer therapeutic in response to a molecular trigger in vivo. *Nat. Biotechnol.* **2018**, *36* (3), 258−264.
(36) Ge, H.; Wang, D.; Pan, Y.; Guo, Y.; Li, H.; Zhang, F.; Zhu, X.; Li, Y.; Zhang, C.; Huang, L. Sequence-Dependent DNA Functionalization of Upconversion Nanoparticles and Their Programmable Assemblies. *Angew. Chem., Int. Ed.* **2020**, *59* (21), 8133−8137.
(37) Jungmann, R.; Steinhauer, C.; Scheible, M.; Kuzyk, A.; Tinnefeld, P.; Simmel, F. C. Single-Molecule Kinetics and Super-Resolution Microscopy by Fluorescence Imaging of Transient Binding on DNA Origami. *Nano Lett.* **2010**, *10* (11), 4756−4761.
(38) Jungmann, R.; Avendaño, M. S.; Woehrstein, J. B.; Dai, M.; Shih, W. M.; Yin, P. Multiplexed 3D cellular super-resolution imaging with DNA-PAINT and Exchange-PAINT. *Nat. Methods* **2014**, *11* (3), 313−318.
(39) Schueder, F.; Lara-Gutiérrez, J.; Beliveau, B. J.; Saka, S. K.; Sasaki, H. M.; Woehrstein, J. B.; Strauss, M. T.; Grabmayr, H.; Yin, P.; Jungmann, R. Multiplexed 3D super-resolution imaging of whole cells using spinning disk confocal microscopy and DNA-PAINT. *Nat. Commun.* **2017**, *8*, 2090.
(40) Strauss, M. T.; Schueder, F.; Haas, D.; Nickels, P. C.; Jungmann, R. Quantifying absolute addressability in DNA origami with molecular resolution. *Nat. Commun.* **2018**, *9*, 1600.
(41) Hahn, J.; Chou, L. Y. T.; Sørensen, R. S.; Guerra, R. M.; Shih, W. M. Extrusion of RNA from a DNA-Origami-Based Nanofactory. *ACS Nano* **2020**, *14* (2), 1550−1559.
(42) Wade, O. K.; Woehrstein, J. B.; Nickels, P. C.; Strauss, S.; Stehr, F.; Stein, J.; Schueder, F.; Strauss, M. T.; Ganji, M.; Schnitzbauer, J.; Grabmayr, H.; Yin, P.; Schwille, P.; Jungmann, R. 124-Color Super-resolution Imaging by Engineering DNA-PAINT Blinking Kinetics. *Nano Lett.* **2019**, *19* (4), 2641−2646.
(43) Schueder, F.; Stein, J.; Stehr, F.; Auer, A.; Sperl, B.; Strauss, M. T.; Schwille, P.; Jungmann, R. An order of magnitude faster DNA-PAINT imaging by optimized sequence design and buffer conditions. *Nat. Methods* **2019**, *16* (11), 1101−1104.
(44) Strauss, S.; Jungmann, R. Up to 100-fold speed-up and multiplexing in optimized DNA-PAINT. *Nat. Methods* **2020**, *17* (8), 789−791.
(45) Kempter, S.; Khmelinskaia, A.; Strauss, M. T.; Schwille, P.; Jungmann, R.; Liedl, T.; Bae, W. Single Particle Tracking and Super-Resolution Imaging of Membrane-Assisted Stop-and-Go Diffusion and Lattice Assembly of DNA Origami. *ACS Nano* **2019**, *13* (2), 996−1002.
(46) Gür, F. N.; Kempter, S.; Schueder, F.; Sikeler, C.; Urban, M. J.; Jungmann, R.; Nickels, P. C.; Liedl, T. Double- to Single-Strand Transition Induces Forces and Motion in DNA Origami Nanostructures. *Adv. Mater.* **2021**, *33* (37), 2101986.
(47) Scheckenbach, M.; Schubert, T.; Forthmann, C.; Glembockyte, V.; Tinnefeld, P. Self-Regeneration and Self-Healing in DNA Origami Nanostructures. *Angew. Chem., Int. Ed.* **2021**, *60* (9), 4931−4938.
(48) Wang, Y.; Woehrstein, J. B.; Donoghue, N.; Dai, M.; Avendaño, M. S.; Schackmann, R. C. J.; Zoeller, J. J.; Wang, S. S. H.; Tillberg, P. W.; Park, D.; Lapan, S. W.; Boyden, E. S.; Brugge, J. S.; Kaeser, P. S.; Church, G. M.; Agasti, S. S.; Jungmann, R.; Yin, P. Rapid Sequential in Situ Multiplexing with DNA Exchange Imaging in Neuronal Cells and Tissues. *Nano Lett.* **2017**, *17* (10), 6131−6139.
(49) Schlichthaerle, T.; Eklund, A. S.; Schueder, F.; Strauss, M. T.; Tiede, C.; Curd, A.; Ries, J.; Peckham, M.; Tomlinson, D. C.; Jungmann, R. Site-Specific Labeling of Affimers for DNA-PAINT Microscopy. *Angew. Chem., Int. Ed.* **2018**, *57* (34), 11060−11063.
(50) Sograte-Idrissi, S.; Oleksiievets, N.; Isbaner, S.; Eggert-Martinez, M.; Enderlein, J.; Tsukanov, R.; Opazo, F. Nanobody Detection of Standard Fluorescent Proteins Enables Multi-Target DNA-PAINT with High Resolution and Minimal Displacement Errors. *Cells* **2019**, *8* (1), 48.
(51) Filius, M.; Cui, T. J.; Ananth, A. N.; Docter, M. W.; Hegge, J. W.; Van Der Oost, J.; Joo, C. High-Speed Super-Resolution Imaging Using Protein-Assisted DNA-PAINT. *Nano Lett.* **2020**, *20* (4), 2264−2270.
(52) Strauss, S.; Nickels, P. C.; Strauss, M. T.; Jimenez Sabinina, V.; Ellenberg, J.; Carter, J. D.; Gupta, S.; Janjic, N.; Jungmann, R. Modified aptamers enable quantitative sub-10-nm cellular DNA-PAINT imaging. *Nat. Methods* **2018**, *15* (9), 685−688.
(53) Schlichthaerle, T.; Strauss, M. T.; Schueder, F.; Auer, A.; Nijmeijer, B.; Kueblbeck, M.; Jimenez Sabinina, V.; Thevathasan, J. V.; Ries, J.; Ellenberg, J.; Jungmann, R. Direct Visualization of Single Nuclear Pore Complex Proteins Using Genetically-Encoded Probes for DNA-PAINT. *Angew. Chem., Int. Ed.* **2019**, *58* (37), 13004−13008.
(54) Wang, D.-X.; Wang, J.; Wang, Y.-X.; Du, Y.-C.; Huang, Y.; Tang, A.-N.; Cui, Y.-X.; Kong, D.-M. DNA nanostructure-based nucleic acid probes: construction and biological applications. *Chemical Science* **2021**, *12* (22), 7602−7622.
(55) Li, C.; Luo, S.; Wang, J.; Shen, Z.; Wu, Z.-S. Nuclease-resistant signaling nanostructures made entirely of DNA oligonucleotides. *Nanoscale* **2021**, *13* (15), 7034−7051.
(56) Wu, P.; Hwang, K.; Lan, T.; Lu, Y. A DNAzyme-Gold Nanoparticle Probe for Uranyl Ion in Living Cells. *J. Am. Chem. Soc.* **2013**, *135* (14), 5254−5257.
(57) Torabi, S. F.; Wu, P.; McGhee, C. E.; Chen, L.; Hwang, K.; Zheng, N.; Cheng, J.; Lu, Y. In vitro selection of a sodium-specific DNAzyme and its application in intracellular sensing. *Proc. Natl. Acad. Sci. U. S. A.* **2015**, *112* (19), 5903−5908.
(58) Li, L.; Feng, J.; Fan, Y.; Tang, B. Simultaneous imaging of Zn(2+) and Cu(2+) in living cells based on DNAzyme modified gold nanoparticle. *Anal. Chem.* **2015**, *87* (9), 4829−4835.
(59) Qiu, L.; Zhang, T.; Jiang, J.; Wu, C.; Zhu, G.; You, M.; Chen, X.; Zhang, L.; Cui, C.; Yu, R.; Tan, W. Cell membrane-anchored biosensors for real-time monitoring of the cellular microenvironment. *J. Am. Chem. Soc.* **2014**, *136* (38), 13090−13093.
(60) Yang, Z.; Loh, K. Y.; Chu, Y.-T.; Feng, R.; Satyavolu, N. S. R.; Xiong, M.; Nakamata Huynh, S. M.; Hwang, K.; Li, L.; Xing, H.; Zhang, X.; Chemla, Y. R.; Gruebele, M.; Lu, Y. Optical Control of Metal Ion Probes in Cells and Zebrafish Using Highly Selective DNAzymes Conjugated to Upconversion Nanoparticles. *J. Am. Chem. Soc.* **2018**, *140* (50), 17656−17665.
(61) Lin, Y.; Yang, Z.; Lake, R. J.; Zheng, C.; Lu, Y. Enzyme-Mediated Endogenous and Bioorthogonal Control of a DNAzyme Fluorescent Sensor for Imaging Metal Ions in Living Cells. *Angew. Chem., Int. Ed.* **2019**, *58* (47), 17061−17067.
(62) Xiao, M.; Lai, W.; Man, T.; Chang, B.; Li, L.; Chandrasekaran, A. R.; Pei, H. Rationally Engineered Nucleic Acid Architectures for Biosensing Applications. *Chem. Rev.* **2019**, *119* (22), 11631−11717.
(63) Meng, H. M.; Liu, H.; Kuai, H.; Peng, R.; Mo, L.; Zhang, X. B. Aptamer-integrated DNA nanostructures for biosensing, bioimaging and cancer therapy. *Chem. Soc. Rev.* **2016**, *45* (9), 2583−2602.
(64) Zheng, X.; Peng, R.; Jiang, X.; Wang, Y.; Xu, S.; Ke, G.; Fu, T.; Liu, Q.; Huan, S.; Zhang, X. Fluorescence Resonance Energy Transfer-Based DNA Nanoprism with a Split Aptamer for Adenosine Triphosphate Sensing in Living Cells. *Anal. Chem.* **2017**, *89* (20), 10941−10947.

https://doi.org/10.1021/acsabm.2c00128
ACS Appl. Bio Mater. XXXX, XXX, XXX−XXX

(65) Zhao, J.; Gao, J.; Xue, W.; Di, Z.; Xing, H.; Lu, Y.; Li, L. Upconversion Luminescence-Activated DNA Nanodevice for ATP Sensing in Living Cells. *J. Am. Chem. Soc.* **2018**, *140* (2), 578−581.
(66) Peng, P.; Du, Y.; Zheng, J.; Wang, H.; Li, T. Reconfigurable Bioinspired Framework Nucleic Acid Nanoplatform Dynamically Manipulated in Living Cells for Subcellular Imaging. *Angew. Chem., Int. Ed.* **2019**, *58* (6), 1648−1653.
(67) Cheglakov, Z.; Cronin, T. M.; He, C.; Weizmann, Y. Live Cell MicroRNA Imaging Using Cascade Hybridization Reaction. *J. Am. Chem. Soc.* **2015**, *137* (19), 6116−6119.
(68) Karunanayake Mudiyanselage, A.; Yu, Q.; Leon-Duque, M. A.; Zhao, B.; Wu, R.; You, M. Genetically Encoded Catalytic Hairpin Assembly for Sensitive RNA Imaging in Live Cells. *J. Am. Chem. Soc.* **2018**, *140* (28), 8739−8745.
(69) Liang, C. P.; Ma, P. Q.; Liu, H.; Guo, X.; Yin, B. C.; Ye, B. C. Rational Engineering of a Dynamic, Entropy-Driven DNA Nanomachine for Intracellular MicroRNA Imaging. *Angew. Chem., Int. Ed. Engl.* **2017**, *56* (31), 9077−9081.
(70) Meng, X.; Dai, W.; Zhang, K.; Dong, H.; Zhang, X. Imaging multiple microRNAs in living cells using ATP self-powered strand-displacement cascade amplification. *Chem. Sci.* **2018**, *9* (5), 1184−1190.
(71) He, L.; Lu, D.; Liang, H.; Xie, S.; Zhang, X.; Liu, Q.; Yuan, Q.; Tan, W. mRNA-Initiated, Three-Dimensional DNA Amplifier Able to Function inside Living Cells. *J. Am. Chem. Soc.* **2018**, *140* (1), 258−263.
(72) Wu, H.; Zhou, W.-J.; Liu, L.; Fan, Z.; Tang, H.; Yu, R.-Q.; Jiang, J.-H. In vivo mRNA imaging based on tripartite DNA probe mediated catalyzed hairpin assembly. *Chem. Commun.* **2020**, *56* (62), 8782−8785.
(73) Liu, R.; Zhang, S.; Zheng, T. T.; Chen, Y. R.; Wu, J. T.; Wu, Z. S. Intracellular Nonenzymatic In Situ Growth of Three-Dimensional DNA Nanostructures for Imaging Specific Biomolecules in Living Cells. *ACS Nano* **2020**, *14* (8), 9572−9584.
(74) Wang, H.; Peng, P.; Wang, Q.; Du, Y.; Tian, Z.; Li, T. Environment-Recognizing DNA-Computation Circuits for the Intracellular Transport of Molecular Payloads for mRNA Imaging. *Angew. Chem., Int. Ed. Engl.* **2020**, *59* (15), 6099−6107.
(75) Xiao, M.; Wang, X.; Li, L.; Pei, H. Stochastic RNA Walkers for Intracellular MicroRNA Imaging. *Anal. Chem.* **2019**, *91* (17), 11253−11258.
(76) Fu, X.; Ke, G.; Peng, F.; Hu, X.; Li, J.; Shi, Y.; Kong, G.; Zhang, X. B.; Tan, W. Size-selective molecular recognition based on a confined DNA molecular sieve using cavity-tunable framework nucleic acids. *Nat. Commun.* **2020**, *11* (1), 1518.
(77) Fan, H.; Bai, H.; Liu, Q.; Xing, H.; Zhang, X.-B.; Tan, W. Monitoring Telomerase Activity in Living Cells with High Sensitivity Using Cascade Amplification Reaction-Based Nanoprobe. *Anal. Chem.* **2019**, *91* (20), 13143−13151.
(78) Pavlov, V.; Xiao, Y.; Gill, R.; Dishon, A.; Kotler, M.; Willner, I. Amplified Chemiluminescence Surface Detection of DNA and Telomerase Activity Using Catalytic Nucleic Acid Labels. *Anal. Chem.* **2004**, *76* (7), 2152−2156.
(79) Herbert, B.-S.; Hochreiter, A. E.; Wright, W. E.; Shay, J. W. Nonradioactive detection of telomerase activity using the telomeric repeat amplification protocol. *Nat. Protoc.* **2006**, *1* (3), 1583−1590.
(80) Tian, L.; Weizmann, Y. Real-Time Detection of Telomerase Activity Using the Exponential Isothermal Amplification of Telomere Repeat Assay. *J. Am. Chem. Soc.* **2013**, *135* (5), 1661−1664.
(81) Guo, X.; Wu, X.; Sun, M.; Xu, L.; Kuang, H.; Xu, C. Tetrahedron Probes for Ultrasensitive In Situ Detection of Telomerase and Surface Glycoprotein Activity in Living Cells. *Anal. Chem.* **2020**, *92* (2), 2310−2315.
(82) Shen, R.; Zou, L.; Wu, S.; Li, T.; Wang, J.; Liu, J.; Ling, L. A novel label-free fluorescent detection of histidine based upon Cu(2+)-specific DNAzyme and hybridization chain reaction. *Spectrochim Acta A Mol. Biomol Spectrosc* **2019**, *213*, 42−47.
(83) McConnell, E. M.; Cozma, I.; Mou, Q.; Brennan, J. D.; Lu, Y.; Li, Y. Biosensing with DNAzymes. *Chem. Soc. Rev.* **2021**, *50* (16), 8954−8994.
(84) Kong, R. M.; Zhang, X. B.; Chen, Z.; Meng, H. M.; Song, Z. L.; Tan, W.; Shen, G. L.; Yu, R. Q. Unimolecular catalytic DNA biosensor for amplified detection of L-histidine via an enzymatic recycling cleavage strategy. *Anal. Chem.* **2011**, *83* (20), 7603−7607.
(85) Meng, H.-M.; Zhang, X.; Lv, Y.; Zhao, Z.; Wang, N.-N.; Fu, T.; Fan, H.; Liang, H.; Qiu, L.; Zhu, G.; Tan, W. DNA Dendrimer: An Efficient Nanocarrier of Functional Nucleic Acids for Intracellular Molecular Sensing. *ACS Nano* **2014**, *8* (6), 6171−6181.
(86) He, J.-L.; Zhang, Y.; Yang, C.; Huang, S.-Y.; Wu, L.; Mei, T.-T.; Wang, J.; Cao, Z. Hybridization chain reaction based DNAzyme fluorescent sensor for l-histidine assay. *Analytical Methods* **2019**, *11* (16), 2204−2210.
(87) Xu, Y. T.; Ruan, Y. F.; Wang, H. Y.; Yu, S. Y.; Yu, X. D.; Zhao, W. W.; Chen, H. Y.; Xu, J. J. A Practical Electrochemical Nanotool for Facile Quantification of Amino Acids in Single Cell. *Small* **2021**, *17* (26), 2100503.
(88) Jiang, D.; Sun, Y.; Li, J.; Li, Q.; Lv, M.; Zhu, B.; Tian, T.; Cheng, D.; Xia, J.; Zhang, L.; Wang, L.; Huang, Q.; Shi, J.; Fan, C. Multiple-Armed Tetrahedral DNA Nanostructures for Tumor-Targeting, Dual-Modality in Vivo Imaging. *ACS Appl. Mater. Interfaces* **2016**, *8* (7), 4378−4384.
(89) Wang, L.; Jacobson, O.; Avdic, D.; Rotstein, B. H.; Weiss, I. D.; Collier, L.; Chen, X.; Vasdev, N.; Liang, S. H. Ortho-Stabilized (18) F-Azido Click Agents and their Application in PET Imaging with Single-Stranded DNA Aptamers. *Angew. Chem., Int. Ed. Engl.* **2015**, *54* (43), 12777−12781.
(90) Zhu, H.; Zhang, L.; Liu, Y.; Zhou, Y.; Wang, K.; Xie, X.; Song, L.; Wang, D.; Han, C.; Chen, Q. Aptamer-PEG-modified Fe3O4@Mn as a novel T1- and T2- dual-model MRI contrast agent targeting hypoxia-induced cancer stem cells. *Sci. Rep* **2016**, *6*, 39245.
(91) Kim, D.; Jeong, Y. Y.; Jon, S. A Drug-Loaded Aptamer-Gold Nanoparticle Bioconjugate for Combined CT Imaging and Therapy of Prostate Cancer. *ACS Nano* **2010**, *4* (7), 3689−3696.
(92) Zhang, J.; Smaga, L. P.; Satyavolu, N. S. R.; Chan, J.; Lu, Y. DNA Aptamer-Based Activatable Probes for Photoacoustic Imaging in Living Mice. *J. Am. Chem. Soc.* **2017**, *139* (48), 17225−17228.
(93) Peng, R.; Zheng, X.; Lyu, Y.; Xu, L.; Zhang, X.; Ke, G.; Liu, Q.; You, C.; Huan, S.; Tan, W. Engineering a 3D DNA-Logic Gate Nanomachine for Bispecific Recognition and Computing on Target Cell Surfaces. *J. Am. Chem. Soc.* **2018**, *140* (31), 9793−9796.
(94) Zhou, Z.; Fan, D.; Wang, J.; Sohn, Y. S.; Nechushtai, R.; Willner, I. Triggered Dimerization and Trimerization of DNA Tetrahedra for Multiplexed miRNA Detection and Imaging of Cancer Cells. *Small* **2021**, *17* (6), No. e2007355.
(95) Chang, X.; Zhang, C.; Lv, C.; Sun, Y.; Zhang, M.; Zhao, Y.; Yang, L.; Han, D.; Tan, W. Construction of a Multiple-Aptamer-Based DNA Logic Device on Live Cell Membranes via Associative Toehold Activation for Accurate Cancer Cell Identification. *J. Am. Chem. Soc.* **2019**, *141* (32), 12738−12743.
(96) Zhao, H.; Lv, J.; Li, F.; Zhang, Z.; Zhang, C.; Gu, Z.; Yang, D. Enzymatical biomineralization of DNA nanoflowers mediated by manganese ions for tumor site activated magnetic resonance imaging. *Biomaterials* **2021**, *268*, 120591.
(97) Kim, J.; Yu, A. M.; Kubelick, K. P.; Emelianov, S. Y. Gold nanoparticles conjugated with DNA aptamer for photoacoustic detection of human matrix metalloproteinase-9. *Photoacoustics* **2022**, *25*, 100307.
(98) Hu, Q.; Li, H.; Wang, L.; Gu, H.; Fan, C. DNA Nanotechnology-Enabled Drug Delivery Systems. *Chem. Rev.* **2019**, *119* (10), 6459−6506.

https://doi.org/10.1021/acsabm.2c00128
ACS Appl. Bio Mater. XXXX, XXX, XXX−XXX